Acta Geochim (2018) 37(1):134–150
https://doi.org/10.1007/s11631-017-0193-z

ORIGINAL ARTICLE

Elemental characteristics and paleoenvironment reconstruction: a case study of the Triassic lacustrine Zhangjiatan oil shale, southern Ordos Basin, China

Delu Li[1] · Rongxi Li[1] · Zengwu Zhu[2] · Xiaoli Wu[1] · Futian Liu[1] · Bangsheng Zhao[1] · Jinghua Cheng[1] · Baoping Wang[3]

Received: 7 April 2017 / Revised: 10 May 2017 / Accepted: 16 June 2017 / Published online: 6 July 2017

Abstract Using trace elements to reconstruct paleoenvironment is a current hot topic in geochemistry. Through analytical tests of oil yield, ash yield, calorific value, total sulfur, major elements, trace elements, and X-ray diffraction, the quality, mineral content, occurrence mode of elements, and paleoenvironment of the Zhangjiatan oil shale of the Triassic Yanchang Formation in the southern Ordos Basin were studied. The analyses revealed relatively high oil yield (average 6.63%) and medium quality. The mineral content in the oil shale was mainly clay minerals, quartz, feldspar, and pyrite; an illite–smectite mixed layer comprised the major proportion of clay minerals. Compared with marine oil shale in China, the Zhangjiatan oil shale had higher contents of quartz, feldspar, and clay minerals, and lower calcite content. Silica was mainly in quartz and Fe was associated with organic matter, which is different from marine oil shale. The form of calcium varied. Cluster analyses indicated that Fe, Cu, U, V, Zn, As, Cs, Cd, Mo, Ga, Pb, Co, Ni, Cr, Sc, P, and Mn are associated with organic matter while Ca, Na, Sr, Ba, Si, Zr, K, Al, B, Mg, and Ti are mostly terrigenous. Sr/Cu, Ba/Al, V/(V + Ni), U/Th, AU, and δU of oil shale samples suggest the paleoclimate was warm and humid, paleoproductivity of the lake was relatively high during deposition of the shale—which mainly occurred in fresh water—and the paleo-redox condition was dominated by reducing conditions. Fe/Ti ratios of the oil shale samples suggest clear hydrothermal influence in the eastern portion of the study area and less conspicuous hydrothermal influence in the western portion.

Keywords Trace elements · Occurrence mode · Paleoenvironment · Zhangjiatan oil shale · Yanchang Formation · Ordos Basin

1 Introduction

Oil shale, as one of the most important unconventional petroleum resources, has attracted much attention in recent years (Liu and Liu 2005; Lü et al. 2015; Hakimi et al. 2016; Song et al. 2016). In general, shale with over 3.5% oil yield is defined as oil shale, and can release thermal energy and shale oil by low temperature carbonization (Fu et al. 2015; Liu et al. 2015). Prior research on oil shale has mainly focused on the marine environment, especially in northern China—including the Cretaceous oil shale in Qiangtang Basin (Fu et al. 2007, 2010a, b, 2015, 2016; Wang et al. 2010), middle-upper Neoproterozoic oil shale in Yanshan Region (Bian et al. 2005; Liu et al. 2011), etc. Based on elemental geochemistry, the oil shale in Qiangtang Basin was deposited in a tropical-subtropical environment (Fu et al. 2009; Wang et al. 2010). The Qiangtang oil shale formed at the edge of a gulf-lagoon, with fresh water input and high paleoproductivity (Fu et al. 2007; Wang et al. 2010); petrography and geochemistry indicate that hydrothermal fluid has impacted its formation (Sun et al. 2003; Chen and Sun 2004; Chen et al. 2004). Major and trace element analyses suggest hydrothermal activity was frequent during sedimentation of the Xiamaling Formation oil shale in the middle-upper Neoproterozoic (Sun et al. 2003). Lacustrine oil shale is widely distributed

✉ Rongxi Li
Rongxi99@163.com

[1] School of Earth Sciences and Resources, Chang'an University, Xi'an 710054, China

[2] Shaanxi Center of Geological Survey, Xi'an 710068, China

[3] Yanchang Oilfiled Co.,Ltd, Yan'an 716000, China

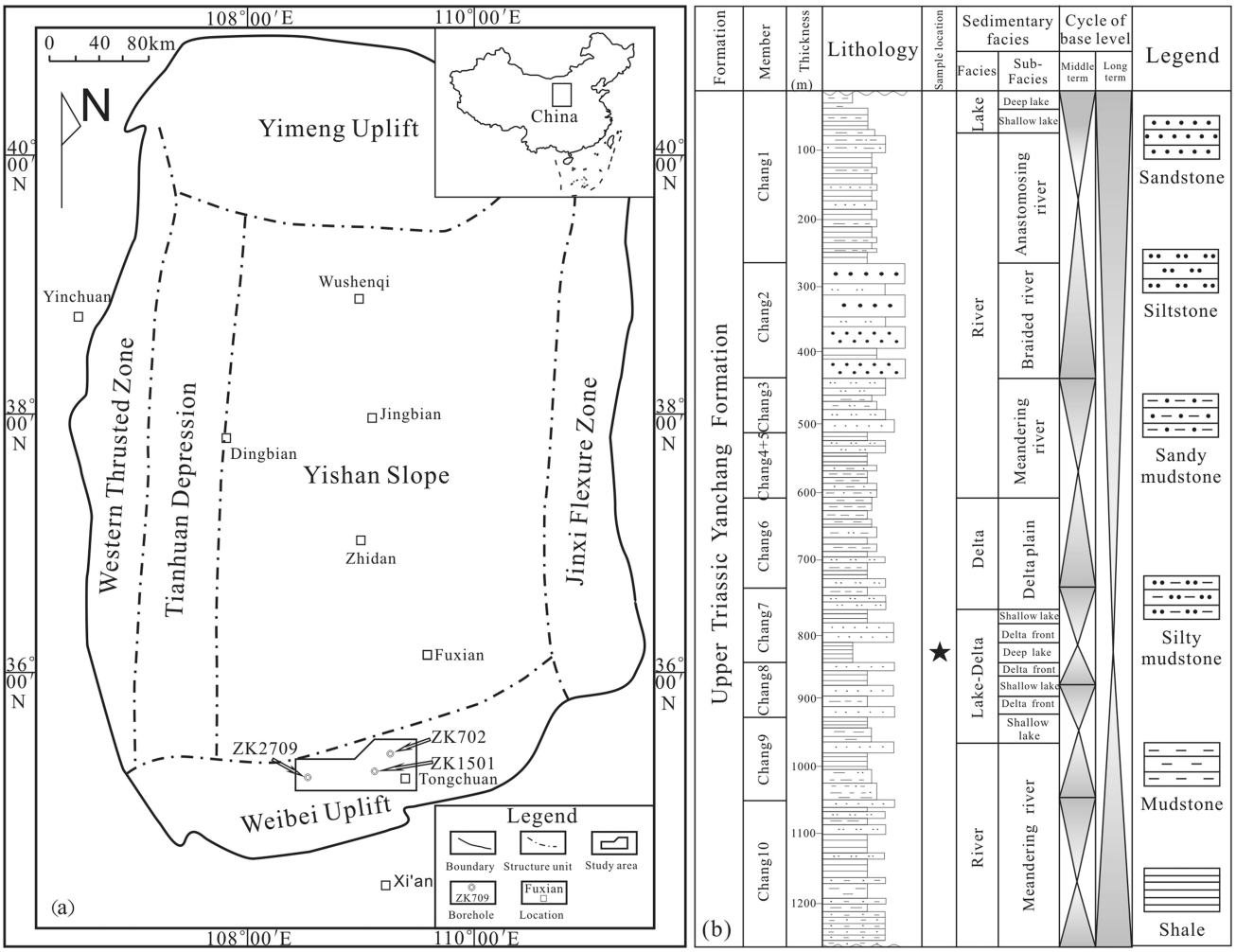

Fig. 1 **a** Geologic map of the Ordos Basin and location of studied section (Li et al. 2016) and **b** stratigraphic column of Upper Triassic Yanchang Formation in study area (modified after Qiu et al. 2014)

across China (Bai and Wu 2006; Bai et al. 2015; Liu et al. 2006). However, most previous studies have concentrated on calculating reserves (Bai and Wu 2006; Bai et al. 2009; Lu et al. 2006). Elemental and mineral characteristics of lacustrine oil shales, and implications for paleoenvironment, are badly in need of additional investigation.

A typical lacustrine oil shale in China, the Zhangjiatan oil shale of the Triassic Yanchang Formation in the southern Ordos Basin has many merits, such as wide distribution, abundance, and shallow burial (Lu et al. 2006; Bai et al. 2009; Li et al. 2009a, b, 2014; Chang et al. 2012; Wang and Yan, 2012; Deng et al. 2013; Luo et al. 2014). Organic geochemistry analyses show that the Zhangjiatan oil shale in Chang 7 Member of the Yanchang Formation is dominated by organic matter type II_1 and approaches mature designation (Liu et al. 2009; Ma et al. 2016; Wei et al. 2016). However, few studies have focused on elemental geochemistry of the oil shale, particularly occurrence of trace elements. Although faunal data, framboidal pyrite, and the ratio of organic carbon to total phosphorus in the oil shale indicate deposition was dominated by oxidizing conditions (Yang et al. 2010; Yuan et al. 2016), biomarkers have shown reducing conditions (Deng et al. 2013). Additionally, discussions of oil shale paleosalinity are still unsettled (Luo et al. 2014), with a possible marine transgression event in the southern Ordos Basin. Elemental geochemistry of some oil shale outcrop samples, focusing on Tongchuan City in southern Ordos Basin, has improved understanding of the paleoenvironment (Sun et al. 2015). However, two concentrated oil shale samples from one location do not necessarily reflect the entire southern Ordos Basin as weathering and alteration can significantly impact elemental characteristics of samples.

In order to improve understanding, we evaluated the quality of oil shale and the occurrence mode of trace elements. Then, by using the specific or calculated value, paleoenvironment was reconstructed. Finally, relationships

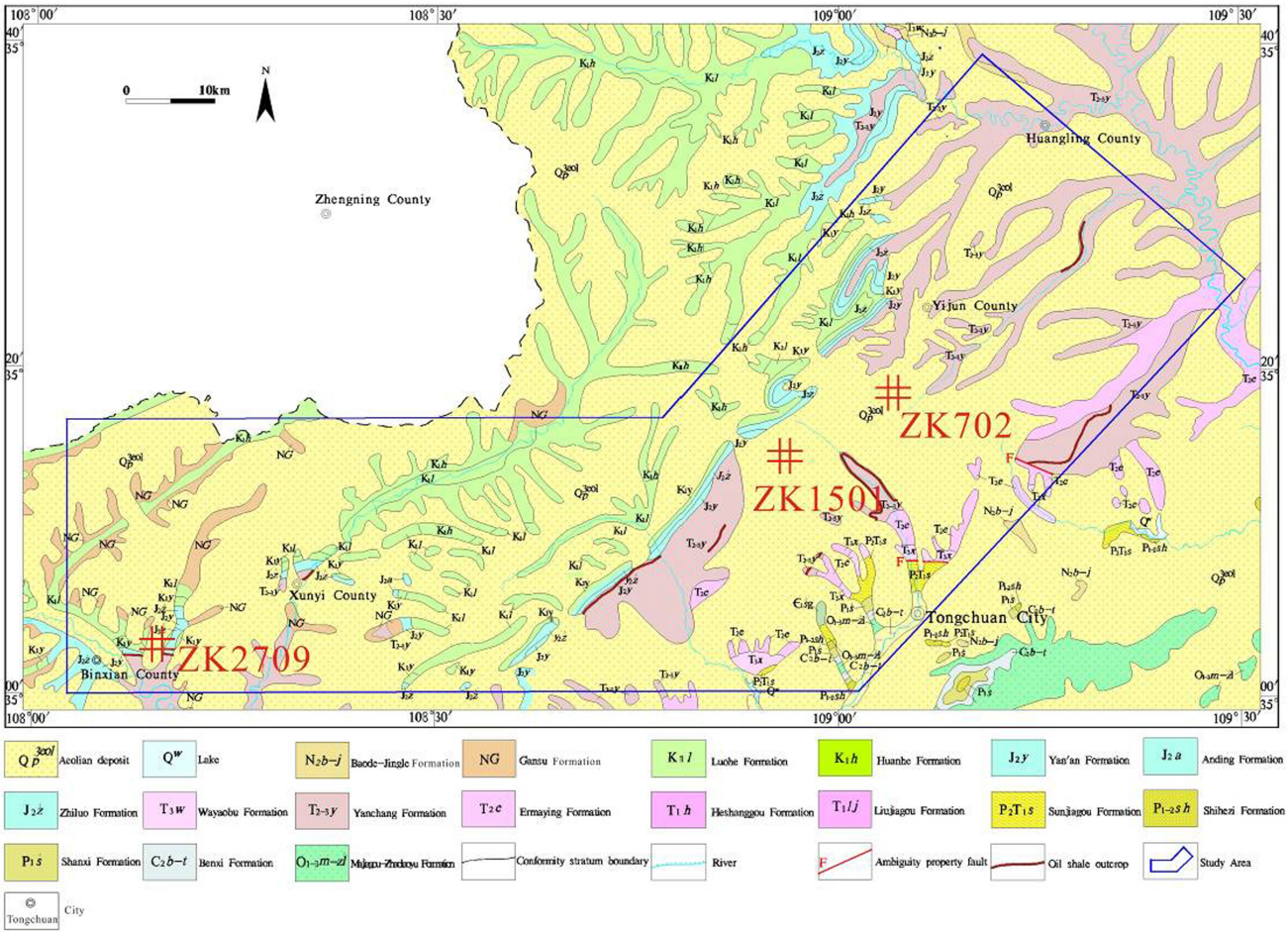

Fig. 2 Simplified geologic map of study area, showing the location of drill holes (modified after Ma et al. 2016)

between single elements and paleoenvironment were analyzed to determine the indicators of paleoenvironment of the lacustrine oil shale. This study fills gaps of lacustrine oil shale elemental geochemistry in the southern Ordos Basin and should help guide future exploration.

2 Geologic setting

The Ordos Basin is a superimposed basin with stable deposition and multiple sedimentary cycles (Fig. 1a) located in mid-western China (Liu et al. 2008). The Ordos formed as a marine basin of the North China Block by the Carboniferous to Permian and has a Proterozoic crystalline basement (Wan et al. 2013; Qiu et al. 2015). After the Triassic, the basin gradually departed from the North China Block and evolved into a large inland sedimentary basin with a relatively quiet tectonic setting (Li et al. 2006, 2008). Affected by the Indosinian Orogeny, the whole basin gradually uplifted and subducted in the Early Cretaceous and underwent reformation. According to present tectonic characteristics, basement features and evolutionary history, the basin is divided into six first-order tectonic units: the Weibei Uplift, Yishan Slope, Yimeng Uplift, Jinxi Flexure Zone, Tianhuan Depression, and Western Thrusted Zone. The Triassic Yanchang Formation went through an integrated occurrence-extinction period and deposited a set of progradation aggradation retrogradation strata with a thickness of 1000–1300 m (Wu et al. 2004; Li et al. 2009a, b; Zou et al. 2012). According to sedimentary cycles and rock assemblages, the Yanchang Formation can be further divided into 10 Members: Chang 10 to Chang 1 (Qiu et al. 2010). During the initial stage of Chang 7, due to extension and sinking of the basin along with orogenies and paroxysmal eruption in the south, the lake reached its largest size (Qiu et al. 2015). There are two sets of oil shale in the Yanchang Formation, namely the Zhangjiatan at the bottom of Chang 7 with a thickness of 20–30 m (Wang and Yan 2012) and the Lijiapan (Wang and Yan 2012; Dong et al. 2014) at the top of Chang 9 with a thickness of 5–15 m. The Zhangjiatan is the main Mesozoic oil reservoir in the Ordos Basin (He 2003; Deng et al. 2013; Li et al. 2016).

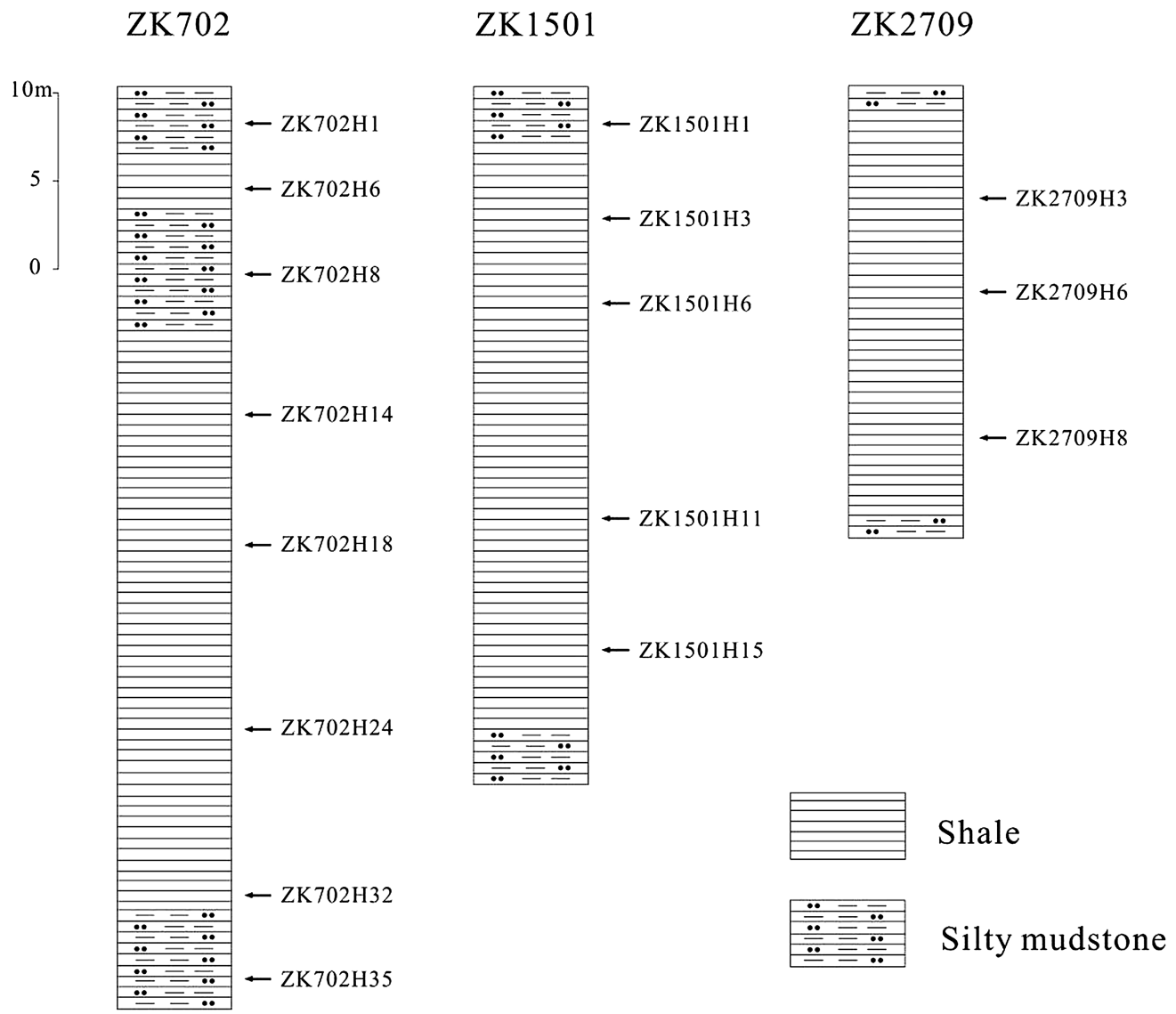

Fig. 3 Zhangjiatan oil shale sections, showing sampling locations

The study area is located in the Weibei Uplift, southern Ordos Basin. Due to the Indosinian Orogeny in the Late Triassic and the later Yanshan Orogeny, the study area experienced unbalanced uplift and lacks upper Yanchang strata. The bottom of Chang 7 contains oil shale, shale, mudstone, and silty mudstone (Fig. 1b). Shallow burial conditions and the significant thickness of the Zhangjiatan make it economically viable. Understanding the Zhangjiatan may improve oil shale exploration.

3 Samples and analytical methods

A total of 16 samples were collected from three oil shale sections in the lower Chang 7 Member in the southern Ordos Basin (Figs. 2, 3). All samples were analyzed for oil yield (T_{ad}), ash yield (A_d), calorific value ($Q_{b,ad}$), total sulfur ($S_{t,d}$), major element oxides, and trace elements. Four samples were tested by X-ray diffraction (XRD) for mineral content.

For the oil yield analysis, samples were ground to a particle size of less than 3 mm, then 50 g of each sample was enclosed in aluminum retort by low temperature carbonization for analysis. The procedure followed the Chinese standard methods SH/T 0508-1992(1992).

The ash content analysis used the slow-ashing method. Each sample of about 1 g was ground to less than 0.2 mm and tiled to a cupel. Then the cupel was heated to 815 ± 10°C in a muffle furnace until the residue content stabilized. We followed the Chinese standard methods GB/T 212-2008 (2008a, b). Precision was within 5%.

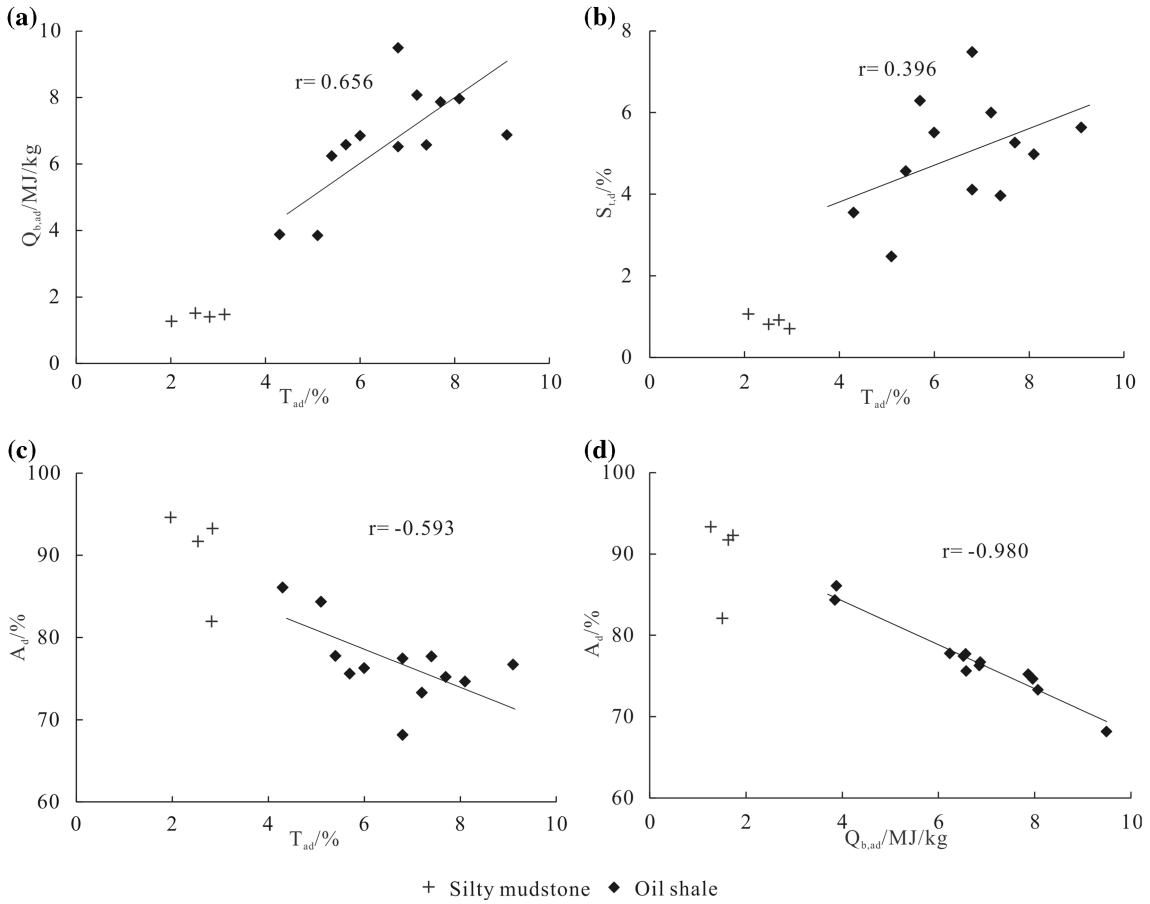

Fig. 4 Relationships between key parameters of oil shale and silty mudstone samples

Table 1 Mineral content tested by XRD in oil shale samples (%)

Sample no.	Quartz	Feldspar			Calcite	Pyrite	Siderite	Ankerite	Gypsum	Jarosite	Clay minerals
		Potassium feldspar	Anorthose	Buddingtonite							
ZK702H14	24.7		9.6	6.2	3.7	19.1			0.4	7.9	28.4
ZK702H24	31.0	9.0	10.0			5.0		4.0			41.0
ZK1501ZH6	24.0	3.0	11.0		5.0	7.0	1.0	3.0			46.0
ZK2709H3	26.0	6.0	10.0		1.0		7.0		8.0		42.0

For the determination of calorific value, samples of 1 g with grain size below 0.2 mm were put into a combustion boat and ignited electrically by oxygen with a purity of more than 99.5%. After 6–7 min, temperatures were recorded for 3 min at 1-min intervals and the highest temperature was recorded as the final temperature. The analytical method followed the Chinese National Standard GB/T 213-2008(GB/T 2008a, b). Analytical error was within 5%.

The samples for total sulfur analysis were powdered to less than 100 μm and heated in a pipe furnace to 1250 ± 20°C with fluxing agent of cupric oxide powder. The method followed Chinese National Standard GB/T 6730.17-2014 (2014).

For mineral content analysis, XRD was performed with a D8 ADVANCE powder diffractometer. The analytical procedures followed Chinese National Standard SY/T 6210-1996(1996) and the precision was within 1%.

The above analyses were conducted at Shaanxi Coal Geological Laboratory Co., Ltd.

The samples for element analysis were all powdered to less than 200 mesh, and analyzed by X-ray fluorescence spectrometry (XRF) for major elements and inductively coupled plasma–mass spectrometry (ICP-MS) for trace

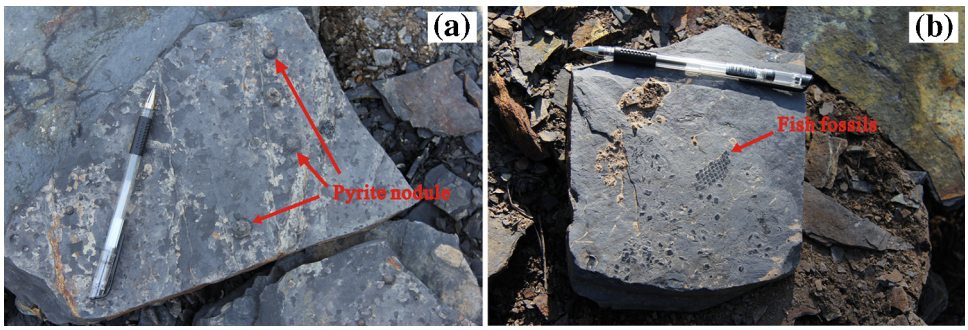

Fig. 5 Zhangjiatan oil shale outcrops of Bawangzhuang Proifle in Tongchuan City, southern Ordos Bain

Table 2 Clay mineral content in oil shale samples (units in %)

Sample no.	Smectite	Illite	Kaolinite	Chlorite	Illite–smectite mixed layer	Chlorite-smectite mixed layer
ZK702H14	0	30	0	1	69	0
ZK702H24	0	33	3	4	60	0
ZK1501ZH6	0	38	5	2	55	0
ZK2709H3	0	14	4	3	79	0

Table 3 Oil yield, calorific value, ash yield, total sulfur, and major elements in oil shale samples (units of Qb,ad are MJ/kg; others are %)

Sample no.	Lithology	T_{ad}	$Q_{b,ad}$	A_d	$S_{t,d}$	SiO_2	Al_2O_3	MgO	CaO	Na_2O	K_2O	P_2O_5	MnO	TiO_2	TFe_2O_3
ZK702H1	Silty mudstone	2.10	1.22	94.39	1.03	68.10	13.06	0.66	1.16	2.32	2.96	0.07	0.03	0.19	1.56
ZK702H6	Oil shale	4.30	3.88	86.08	3.55	55.73	13.54	0.75	0.42	0.98	3.61	0.24	0.09	0.29	4.51
ZK702H8	Silty mudstone	3.00	1.63	93.08	0.53	66.39	12.91	0.60	1.52	1.69	3.04	0.11	0.17	0.19	0.90
ZK702H14	Oil shale	7.20	8.07	73.28	6.00	40.61	13.37	0.97	0.97	0.91	2.25	0.28	0.05	0.40	8.44
ZK702H18	Oil shale	9.10	6.87	76.70	5.63	46.90	10.69	0.86	1.61	1.30	1.85	0.45	0.06	0.36	7.84
ZK702H24	Oil shale	8.10	7.96	74.63	4.98	43.33	12.50	0.98	1.67	1.49	1.49	0.35	0.07	0.33	6.81
ZK702H32	Oil shale	7.70	7.87	75.21	5.26	44.26	12.66	0.93	1.25	1.00	2.37	0.29	0.09	0.34	7.92
ZK702H35	Silty mudstone	2.50	1.56	92.00	0.70	59.95	12.44	1.64	4.56	2.20	4.11	0.17	0.11	0.41	1.22
ZK1501H1	Silty mudstone	2.80	1.50	82.82	0.80	67.38	13.14	0.57	1.25	2.47	2.90	0.11	0.09	0.21	1.42
ZK1501H3	Oil shale	5.70	6.58	75.60	6.29	45.36	11.45	1.06	1.62	1.45	2.12	0.36	0.11	0.39	7.96
ZK1501H6	Oil shale	6.80	9.49	68.15	7.48	36.42	11.37	1.45	2.19	0.74	1.90	0.26	0.08	0.35	9.03
ZK1501H11	Oil shale	6.00	6.85	76.27	5.51	43.58	12.96	1.16	2.36	1.43	2.03	0.41	0.21	0.45	7.43
ZK1501H15	Oil shale	5.40	6.24	77.76	4.56	48.09	14.00	1.22	1.98	1.30	2.36	0.46	0.25	0.39	5.77
ZK2709H3	Oil shale	7.40	6.57	77.71	3.96	44.44	14.15	1.71	1.59	1.29	2.53	0.39	0.19	0.51	6.12
ZK2709H6	Oil shale	6.80	6.52	77.44	4.11	46.51	13.44	1.76	2.09	1.39	2.23	0.38	0.19	0.52	5.40
ZK2709H8	Oil shale	5.10	3.85	84.33	2.47	50.17	15.92	2.01	1.17	1.14	2.80	0.27	0.16	0.63	3.73

T_{ad} = oil yield; $Q_{b,ad}$ = calorific value; A_d = ash yield; $S_{t,d}$ = total sulfur

elements with AA-6800 atomic absorption spectroscopy, UV-2600 ultraviolet–visible spectrophotometer and Perkin Elmer SciexElan 6000. The analytical procedures followed Chinese National Standard GB/T 14506.1 ~ 14-2010(2010) and GB/T 14506.30-2010(2010). Analytical precision was within 5%. The analyses were conducted at the Analytical Center, No. 203 Research Institute of Nuclear Industry.

4 Results

4.1 The industrial quality of shale

In resource assessment of oil shale, four key parameters (oil yield, calorific value, ash yield, and total sulfur) are always considered (Liu et al. 2009). Oil yields of oil shale samples are in the range of 4.3%–9.1% (average 6.63%)

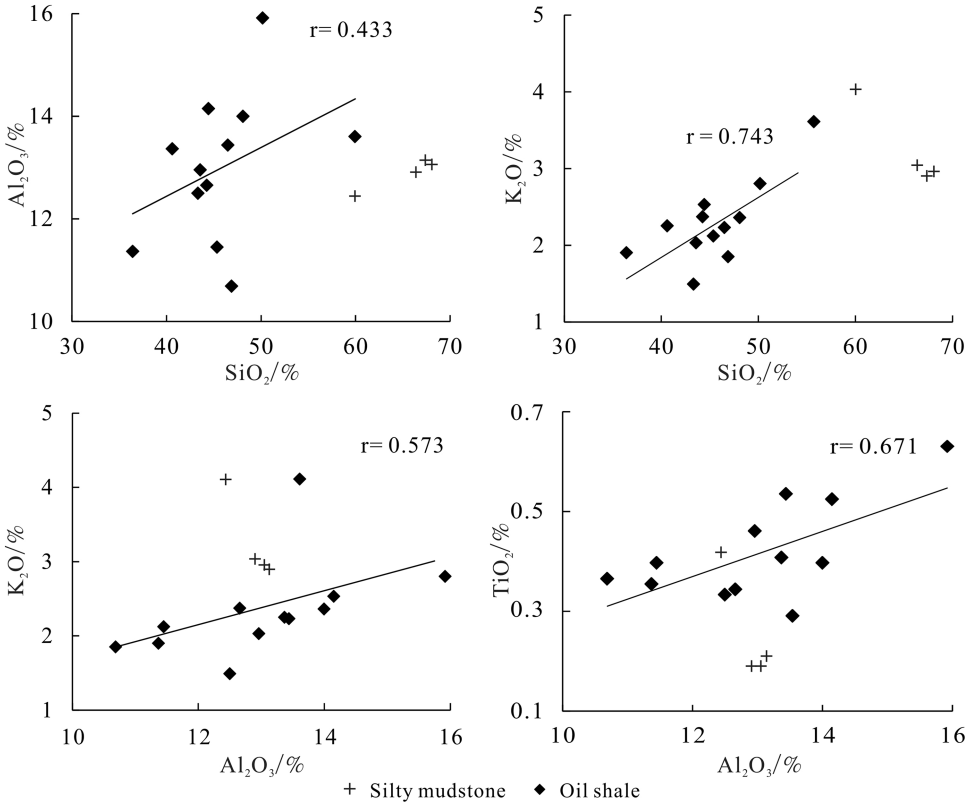

Fig. 6 Relationships among SiO_2, Al_2O_3, K_2O, and TiO_2 concentrations in oil shale and silty mudstone samples

and calorific values are from 3.85 to 9.49 MJ/kg (average 6.73 MJ/kg). The better the quality, the higher the values of the two parameters (Liu et al. 2009; Zhang et al. 2013; Sun et al. 2015). Ash yields of oil shale samples range from 68.15% to 86.08% (average 76.93%) and total sulfur from 2.47% to 7.48% (average 4.98%). The better the quality, the lower the value of these two parameters (Liu et al. 2009; Zhang et al. 2013; Sun et al. 2015). We found that oil yield correlated positively with calorific value (Fig. 4a) and total sulfur (Fig. 4b) and negatively with ash yield (Fig. 4c). Meanwhile, superb negative correlation was observed between calorific value and ash yield (Fig. 4d). According to National Resource Assessment of Oil shale (Dong et al. 2006), oil shale is classified as low, middle, and high grade by oil yield of 3.5%–5%, 5%–10%, and >10%, respectively. Thus, the oil shale in the southern Ordos Basin is middle grade.

4.2 Minerals in oil shale

The minerals identified by XRD in oil shale samples were clay minerals, quartz, feldspar, and pyrite (>5%) with minor amounts of calcite, siderite, ankerite, gypsum, and jarosite (Table 1). Pyrite was mostly in the form of nodules (Fig. 5a). For clay minerals, mixed-layer illite/smectite was predominant, followed by illite (Table 2). Kaolinite and chlorite were measured in trace amounts (Table 2). Compared with marine oil shale, these samples had higher contents of quartz, feldspar, and clay minerals, and much lower average content of calcite (data from 13 marine oil shale samples in Quse Formation of the Early Jurassic, Qiangtang Depression show average quartz: 12.72%; feldspar: 3.38%; clay minerals: 14.28%; calcite: 68.53%,) (Fu et al. 2016). The relatively low calcite and high clay mineral contents are likely associated with terrigenous clastic input (Yu and Zhu, 2013; Zeng et al. 2013, 2014; Xie et al. 2014).

4.3 Major element geochemistry

Major elements can be used to construct associations between elements and minerals in oil shale, as demonstrated by prior study (Fu et al. 2010a, b). Table 3 lists major element concentrations of the oil shale samples. Average contents of SiO_2 (47.28%), Al_2O_3 (13.13%), and TFe_2O_3 (6.00%) were relatively high and the rest were relatively low (<5%). Some major elements show positive correlation with ash yield at 95% confidence level, such as Si ($r = 0.978$), Al ($r = 0.571$), Mg ($r = 0.574$), Ca ($r = 0.397$), Na ($r = 0.683$), K ($r = 0.719$), Mn ($r = 0.123$), and Ti ($r = 0.355$), indicating that these elements have relationships with minerals. P_2O_5 ($r = 0.654$) and TFe_2O_3

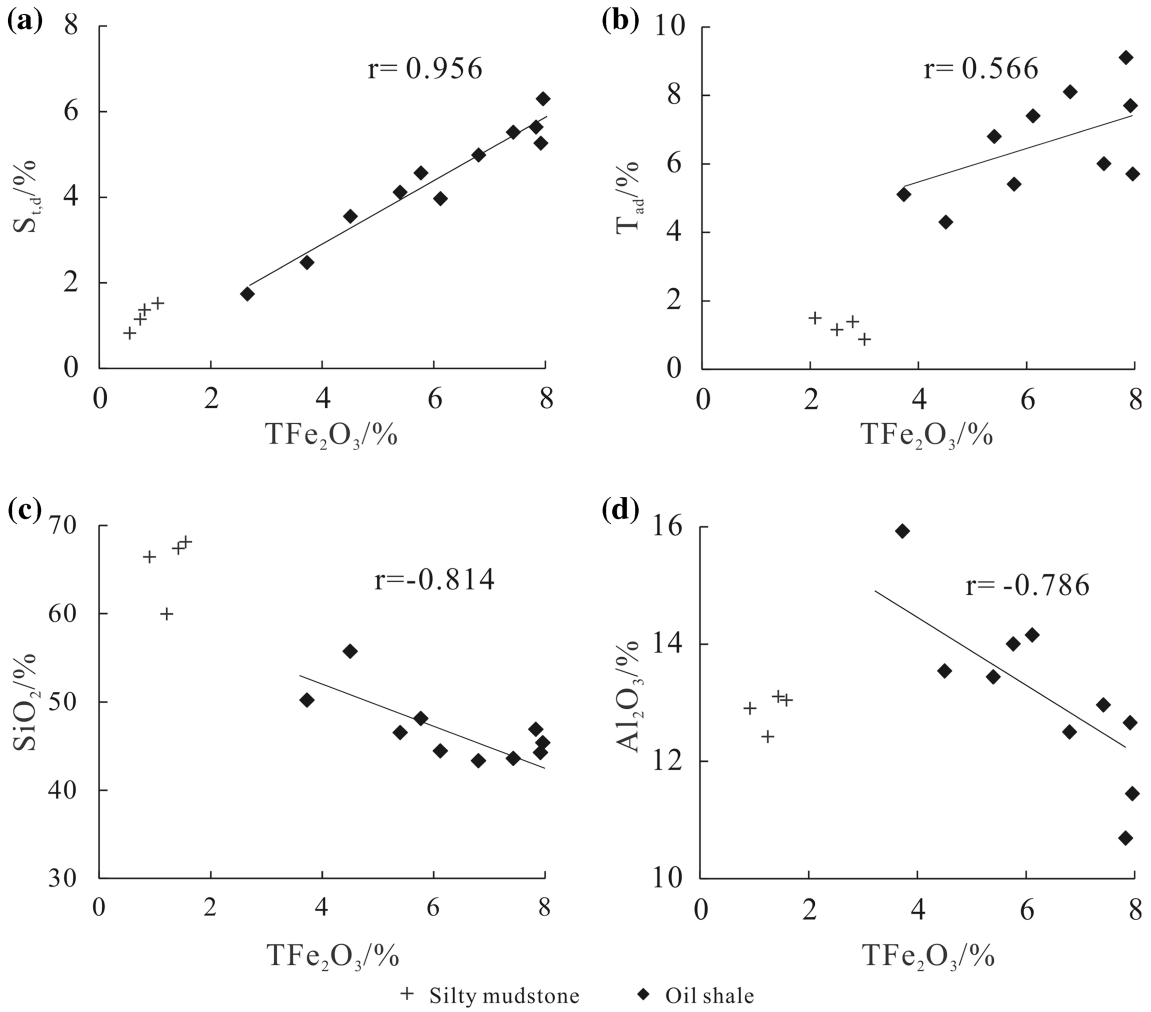

Fig. 7 Relationships between TFe_2O_3 concentration and total sulfur, oil yield, SiO_2, and Al_2O_3 concentrations in oil shale and silty mudstone samples

(r = 0.836) show positive correlation with oil yield, suggesting P and Fe are mainly associated with organic matter.

The elements Si, Al, Ti, and K have some connection with quartz, feldspar, and clay minerals (Fu et al. 2010a,b). Relatively higher correlations among them (Fig. 6) illustrate that they mainly stem from a mixed clay assemblage, in accordance with clay mineral analysis. The Al/Si ratio can reflect the source of SiO_2 (Fu et al. 2010a,b). The Al/Si of oil shale samples varied from 0.26 to 0.37 (average 0.32), implying most SiO_2 is in the form of quartz, with some as clay minerals, which is consistent with the high abundance of quartz in XRD analysis.

The element Fe is generally associated with pyrite in oil shale (Fu et al. 2010a, b). The significantly positive correlation between TFe_2O_3 and total sulfur indicates a high proportion of Fe arising from sulfide oxidation and organic sulfur as the dominant component of total sulfur (Fig. 7a). This is corroborated by the positive correlation between TFe_2O_3 and oil yield (Fig. 7b). TFe_2O_3 showed negative correlations with SiO_2 and Al_2O_3 (Fig. 7c, d), indicating a low frequency of iron in the clay minerals, which contrasts with observations made of marine oil shale (Fu et al. 2010a, b). Moreover, according to XRD, there was a small amount of Fe present as siderite, ankerite, and jarosite, demonstrating the occurrence of segmental Fe.

Calcium presents in various forms (Mukhopadhyay et al. 1998). In marine oil shale, a high abundance of calcite indicates that Ca is associated with calcite (Fu et al. 2016). However, in the Zhangjiatan oil shale samples, the calcite content was relatively low, suggesting different forms of Ca are present. Low correlation (r = 0.396) between CaO and Al_2O_3 suggests presence of Ca not only in clays, but also in other minerals. XRD analysis showed Ca in gypsum. Generally, low CaO content indicates sparse fossil remains in oil shale (Mukhopadhyay et al. 1998). Fish fossil remains observed in Zhangjiatan samples (Fig. 5b) support Ca being of biological origin.

Table 4 Trace element contents (ppm) and corresponding UCC values

Sample no.	Cr	Sr	Zr	Ba	Sc	V	Cu	Zn	Ga	As	Pb	Rb	Cs	Th
ZK702H1	18.30	163.30	125.80	546.30	7.80	43.50	22.60	58.60	18.70	17.90	36.60	169.00	20.30	28.50
ZK702H6	38.90	110.40	138.70	380.90	10.80	123.80	90.30	98.00	22.10	82.40	51.90	215.30	8.33	22.20
ZK702H8	18.30	117.20	111.40	536.40	5.00	39.60	20.90	48.20	17.60	18.90	32.40	189.10	10.60	31.50
ZK702H14	80.40	162.00	120.40	515.70	12.70	282.80	139.20	117.90	23.70	101.60	45.90	107.60	9.72	14.90
ZK702H18	60.20	229.80	135.50	463.40	13.90	235.30	144.50	107.00	19.20	80.10	35.40	88.90	7.88	10.80
ZK702H24	58.10	384.90	132.60	774.60	16.50	305.90	142.10	116.70	22.10	104.40	47.00	82.90	7.56	9.56
ZK702H32	68.40	328.20	146.80	792.60	13.10	316.80	132.30	122.10	24.10	153.30	37.90	117.30	11.30	12.70
ZK702H35	50.90	506.50	159.70	830.60	11.40	82.70	28.90	65.80	18.50	24.80	25.70	142.70	3.79	10.50
ZK1501H1	16.50	137.20	137.50	462.10	7.30	48.60	25.80	57.20	17.10	21.40	36.20	191.30	19.00	31.80
ZK1501H3	56.10	185.00	120.30	562.40	10.10	255.50	139.30	99.80	21.00	81.80	43.80	85.30	10.20	15.80
ZK1501H6	78.60	151.70	116.90	438.50	13.20	286.70	150.10	101.20	22.00	109.20	47.70	81.90	8.57	12.60
ZK1501H11	71.30	438.80	127.20	765.10	16.90	299.70	141.90	121.90	22.50	84.50	48.00	88.70	8.14	9.96
ZK1501H15	55.50	425.00	146.30	849.80	11.60	249.20	123.10	117.80	22.70	113.20	52.80	114.00	9.69	15.10
ZK2709H3	68.60	192.40	127.90	649.50	16.20	189.50	97.50	100.50	19.00	65.60	31.90	115.70	7.70	13.10
ZK2709H6	76.30	182.00	134.00	612.00	14.50	179.00	95.90	95.10	17.90	44.30	29.70	105.00	7.24	12.00
ZK2709H8	78.10	177.70	132.80	662.00	16.60	170.00	64.20	101.00	20.50	37.90	33.60	122.90	8.23	14.00
UCC[a]	35	350	190	550	13.6	60	25	71	17	1.5	20	112	3.7	10.7

Sample no.	U	Co	Ni	Nb	Cd	Hf	Ta	Li	Be	In	Bi	Mo	B
ZK702H1	13.00	6.18	11.90	32.10	0.44	10.10	0.94	36.90	3.00	0.08	0.79	10.10	21.06
ZK702H6	28.50	13.30	22.00	21.70	0.79	7.08	0.97	35.60	3.17	0.08	0.89	44.97	22.81
ZK702H8	16.20	4.37	8.04	25.60	0.21	6.15	0.94	30.80	3.99	0.06	0.91	8.03	15.21
ZK702H14	54.10	21.60	34.20	13.80	0.87	5.17	0.78	43.20	2.47	0.07	0.80	52.32	32.08
ZK702H18	61.30	15.10	29.10	9.20	0.78	4.44	0.86	25.30	1.93	0.06	0.56	76.38	15.51
ZK702H24	61.10	14.60	26.90	7.86	0.75	4.57	0.57	26.70	1.82	0.06	0.48	76.81	14.70
ZK702H32	47.00	14.70	28.30	12.50	0.90	4.84	0.81	25.00	2.56	0.07	0.63	74.14	19.57
ZK702H35	6.80	7.06	15.10	11.10	0.18	3.05	0.38	16.10	2.00	0.05	0.32	10.13	18.91
ZK1501H1	16.50	5.03	9.93	17.70	0.44	5.86	0.90	28.30	3.25	0.05	0.74	12.70	14.50
ZK1501H3	68.20	15.80	27.70	12.30	0.93	4.98	0.72	23.80	2.16	0.06	1.16	52.65	18.44
ZK1501H6	61.70	18.90	31.20	20.00	0.92	4.15	0.52	24.70	1.91	0.06	0.75	24.64	20.86
ZK1501H11	51.10	17.70	30.00	6.69	1.08	3.90	0.54	26.10	2.00	0.06	0.52	58.32	20.00
ZK1501H15	47.30	17.40	31.00	20.00	1.12	6.00	0.66	28.20	2.56	0.08	0.62	62.02	26.56
ZK2709H3	17.70	17.80	36.80	19.90	0.60	5.86	2.11	34.60	2.45	0.08	0.59	14.40	29.50
ZK2709H6	21.60	17.50	36.90	18.10	0.68	5.90	1.76	35.30	2.25	0.07	0.55	23.00	43.80
ZK2709H8	12.70	17.10	36.70	17.40	0.51	5.51	1.52	40.60	2.47	0.08	0.53	25.00	51.00
UCC[a]	2.8	10	20	25	0.098	5.8	2.2	20	3	0.05	0.127	1.5	15

[a] data cited from McLennan (2001)

4.4 Trace element geochemistry

The trace element contents of samples are presented in Table 4. Ba, Sr, V, Zr, Cu, Rb, and Zn were in relatively high abundance (>100 ppm on average). Compared with the average value of the upper continental crust (UCC) (McLennan 2001), As, U, Cd, and Mo were highly enriched, while Sr, Nd, and Ta were depleted. Element enrichment was quantified by the enrichment factor (EF): $EF = (X/Al)_{sample}/(X/Al)_{ucc}$. All analyzed trace elements from oil shale samples were classified into three groups by EF (Fig. 8; Table 5): (1) Cu, As, U, Cd, Bi, and Mo (average EF $\geq$ 5); (2) Cr, Ba, Sc, V, Zn, Ga, Pb, Rb, Cs, Th, Co, Ni, Hf, Li, In, and B (1 $\leq$ average EF $<$ 5); and (3) Sr, Zr, Nb, Ta, and Be (average EF $<$1). In general, Cu is associated with biological growth and Mo with chalcophile elements (Sun et al. 2015). The highly enriched Cu and Mo imply that there was high productivity during oil shale formation. The extremely high U concentration in oil shale is probably due to redox conditions (Cao et al. 2012; Bai et al. 2015).

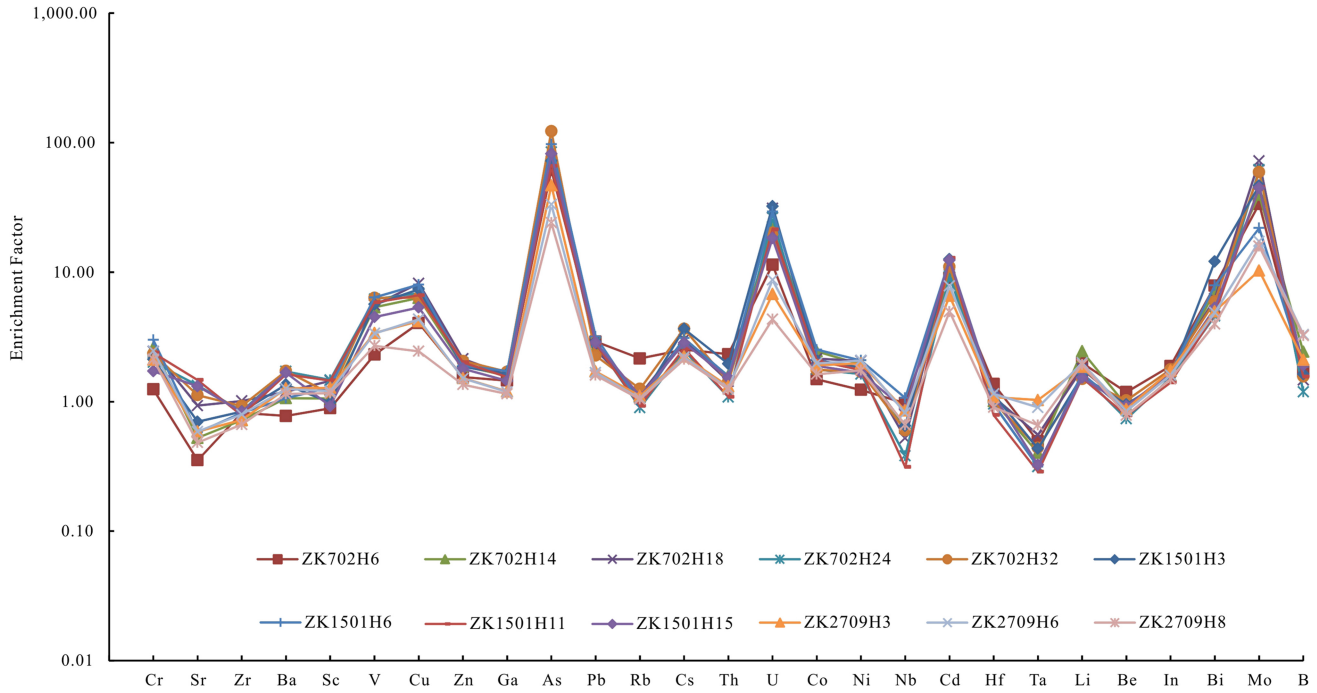

Fig. 8 Spider diagram of trace elements of oil shale samples

Ba content gradually decreases with increased distance from the lakeshore (Sun et al. 1997). In addition, Ba is often associated with paleoproductivity and can reflect organic matter content (Sun et al. 1997). The average EF of Ba (1.34) in this study indicates that the oil shale was deposited in a depocenter with high organic matter.

The Sr EF of oil shale samples was higher than that of mudstone from Chang 6 to Chang 3 in the southern Ordos Basin (EF <1.0; Qiu et al. 2015). Increased Sr is usually associated with increased salinity and calcite (Zhang et al. 2004). This suggests the paleosalinity of southern Ordos Basin water gradually reduced after Chang 7 deposition. In addition, the EF of U in oil shale samples (Table 5) was clearly higher than that in mudstone from Chang 6 to Chang 3 (EF just above 1.0), suggesting that reducibility of water gradually declined. Compared with marine oil shale from Bilong Co in China (Fu et al. 2016), lacustrine oil shale from Chang 7 returned a significantly lower EF of Sr and higher EF of U. The variation of EF may be due to mineral content, water depth, redox conditions, or paleoclimate (Zhang et al. 2004, 2011; Ma et al. 2016).

5 Discussion

5.1 Element associations

Vertical distributions of selected elements are shown in Fig. 9. Compared with silty mudstone, most oil shale samples returned high Cu, U, and V concentrations and low Al and Si concentrations. The variations of Fe, Cu, U, and V roughly paralleled oil yield and total sulfur, indicating that the four elements are closely associated with organic matter. The vertical distributions of Al and Si are similar to that of ash yield, suggesting quartz and clay minerals are the bases of ash yield and Si is present in clay minerals. The element patterns are relatively consistent, indicating that these elements are controlled by a common sedimentary environment (Fu et al. 2010a, b, c).

According to the established sedimentary cycle of the Yanchang Formation, the lake reached its largest scale during oil shale deposition (He 2003), leading to different sedimentary environments between oil shale and silty mudstone. The variation of environment may have influenced the presence of Al and Si.

Correlation coefficients and tree diagrams in cluster analysis help quantify correlations and attribute relationships in samples by grouping samples to optimize within-group similarity (Zhu et al. 2000; Zhao et al. 2015). Statistical Program for Social Sciences (SPSS) version 20.0 developed by IBM was used to analyze element associations. By cluster analysis, trace elements, major elements, total sulfur, oil yield, and ash yield were classified into two groups (Fig. 10).

Group A includes total sulfur, Fe, Cu, U, V, Sr, Ba, Zn, Ga, As, Mo, Pb, Cd, Cs, Na, P, Ca, Mn, and T_{ad}. The correlation coefficients of Fe-Cu (0.918), U-Cu (0.944), and V-Cu (0.847) were all higher than 0.80, indicating a

Table 5 Enrichment factors of trace elements

Sample no.	Cr	Sr	Zr	Ba	Sc	V	Cu	Zn	Ga	As	Pb	Rb	Cs	Th
ZK702H1	0.61	0.54	0.77	1.15	0.67	0.84	1.05	0.96	1.28	13.86	2.13	1.75	6.37	3.09
ZK702H6	1.25	0.35	0.82	0.78	0.89	2.31	4.05	1.55	1.46	61.55	2.91	2.15	2.52	2.32
ZK702H8	0.61	0.39	0.69	1.15	0.43	0.78	0.98	0.80	1.22	14.81	1.90	1.98	3.37	3.46
ZK702H14	2.61	0.53	0.72	1.06	1.06	5.35	6.32	1.88	1.58	76.85	2.60	1.09	2.98	1.58
ZK702H18	2.44	0.93	1.01	1.20	1.45	5.57	8.20	2.14	1.60	75.78	2.51	1.13	3.02	1.43
ZK702H24	2.01	1.33	0.85	1.71	1.47	6.19	6.90	1.99	1.58	84.47	2.85	0.90	2.48	1.08
ZK702H32	2.34	1.12	0.93	1.73	1.15	6.33	6.34	2.06	1.70	122.46	2.27	1.25	3.66	1.42
ZK702H35	1.77	1.76	1.02	1.84	1.02	1.68	1.41	1.13	1.33	20.16	1.57	1.55	1.25	1.20
ZK1501H1	0.54	0.45	0.84	0.97	0.62	0.94	1.19	0.93	1.16	16.47	2.09	1.97	5.93	3.43
ZK1501H3	2.12	0.70	0.84	1.35	0.98	5.64	7.38	1.86	1.64	72.25	2.90	1.01	3.65	1.96
ZK1501H6	3.00	0.58	0.82	1.06	1.29	6.38	8.01	1.90	1.73	97.13	3.18	0.98	3.09	1.57
ZK1501H11	2.38	1.47	0.78	1.63	1.45	5.85	6.64	2.01	1.55	65.94	2.81	0.93	2.58	1.09
ZK1501H15	1.72	1.32	0.83	1.67	0.92	4.50	5.34	1.80	1.45	81.77	2.86	1.10	2.84	1.53
ZK2709H3	2.10	0.59	0.72	1.27	1.28	3.39	4.18	1.52	1.20	46.89	1.71	1.11	2.23	1.31
ZK2709H6	2.46	0.59	0.80	1.26	1.20	3.37	4.33	1.51	1.19	33.33	1.68	1.06	2.21	1.27
ZK2709H8	2.13	0.48	0.67	1.15	1.16	2.70	2.45	1.36	1.15	24.08	1.60	1.05	2.12	1.25
Average	2.21	0.83	0.82	1.32	1.19	4.80	5.84	1.80	1.48	70.21	2.49	1.15	2.78	1.48

Sample no.	U	Co	Ni	Nb	Cd	Hf	Ta	Li	Be	In	Bi	Mo	B
ZK702H1	5.39	0.72	0.69	1.49	5.22	2.02	0.50	2.14	1.16	1.74	7.23	7.82	1.63
ZK702H6	11.40	1.49	1.23	0.97	9.03	1.37	0.49	1.99	1.18	1.88	7.85	33.59	1.70
ZK702H8	6.80	0.51	0.47	1.20	2.52	1.25	0.50	1.81	1.56	1.39	8.42	6.29	1.19
ZK702H14	21.92	2.45	1.94	0.63	10.07	1.01	0.40	2.45	0.93	1.59	7.15	39.58	2.43
ZK702H18	31.07	2.14	2.06	0.52	11.29	1.09	0.55	1.80	0.91	1.70	6.26	72.26	1.47
ZK702H24	26.48	1.77	1.63	0.38	9.29	0.96	0.31	1.62	0.74	1.53	4.59	62.14	1.19
ZK702H32	20.11	1.76	1.70	0.60	11.00	1.00	0.44	1.50	1.02	1.77	5.94	59.23	1.56
ZK702H35	2.96	0.86	0.92	0.54	2.24	0.64	0.21	0.98	0.81	1.20	3.07	8.24	1.54
ZK1501H1	6.80	0.58	0.57	0.82	5.18	1.17	0.47	1.63	1.25	1.15	6.73	9.77	1.12
ZK1501H3	32.27	2.09	1.83	0.65	12.57	1.14	0.43	1.58	0.95	1.56	12.10	46.50	1.63
ZK1501H6	29.40	2.52	2.08	1.07	12.53	0.95	0.32	1.65	0.85	1.65	7.88	21.92	1.86
ZK1501H11	21.36	2.07	1.76	0.31	12.90	0.79	0.29	1.53	0.78	1.40	4.79	45.51	1.56
ZK1501H15	18.30	1.89	1.68	0.87	12.38	1.12	0.33	1.53	0.92	1.65	5.29	44.80	1.92
ZK2709H3	6.78	1.91	1.97	0.85	6.56	1.08	1.03	1.85	0.88	1.74	4.98	10.29	2.11
ZK2709H6	8.71	1.98	2.08	0.82	7.83	1.15	0.90	1.99	0.85	1.60	4.89	17.31	3.30
ZK2709H8	4.32	1.63	1.75	0.66	4.96	0.91	0.66	1.93	0.78	1.50	3.98	15.88	3.24
Average	19.34	1.98	1.81	0.69	10.04	1.05	0.51	1.78	0.90	1.63	6.31	39.08	2.00

$EF = (X/Al)_{sample}/(X/Al)_{ucc}$

close relationship among Fe, Cu, U, and V (Table 6). Elements from this group generally had negative correlation coefficients with ash yield (15 out of 17 elements had negative correlation, with values ranging from −0.890 to 0.277) and generally positive correlation coefficients with oil yield (12 out of 17 elements had positive correlation, with values ranging from −0.424 to 0.566) (Table 6). The positive correlations with oil yield indicate that these elements are mainly associated with organic matter. Previous research has suggested an extremely high positive correlation between total organic carbon and oil shale yield (Liu et al. 2009; Zhang et al. 2013).

Group B includes T_{ad}, Si, K, Rb, Be, In, Hf, Th, Mg, Ti, Ni, B, Cr, Al, Li, Co, Nb, Ta, Bi, Zr, and Sc. These elements generally had positive correlation coefficients with ash yield (13 out of 17 elements had positive correlation, with values ranging from −0.469 to 0.954) and generally negative correlation with oil yield (14 out of 17 elements

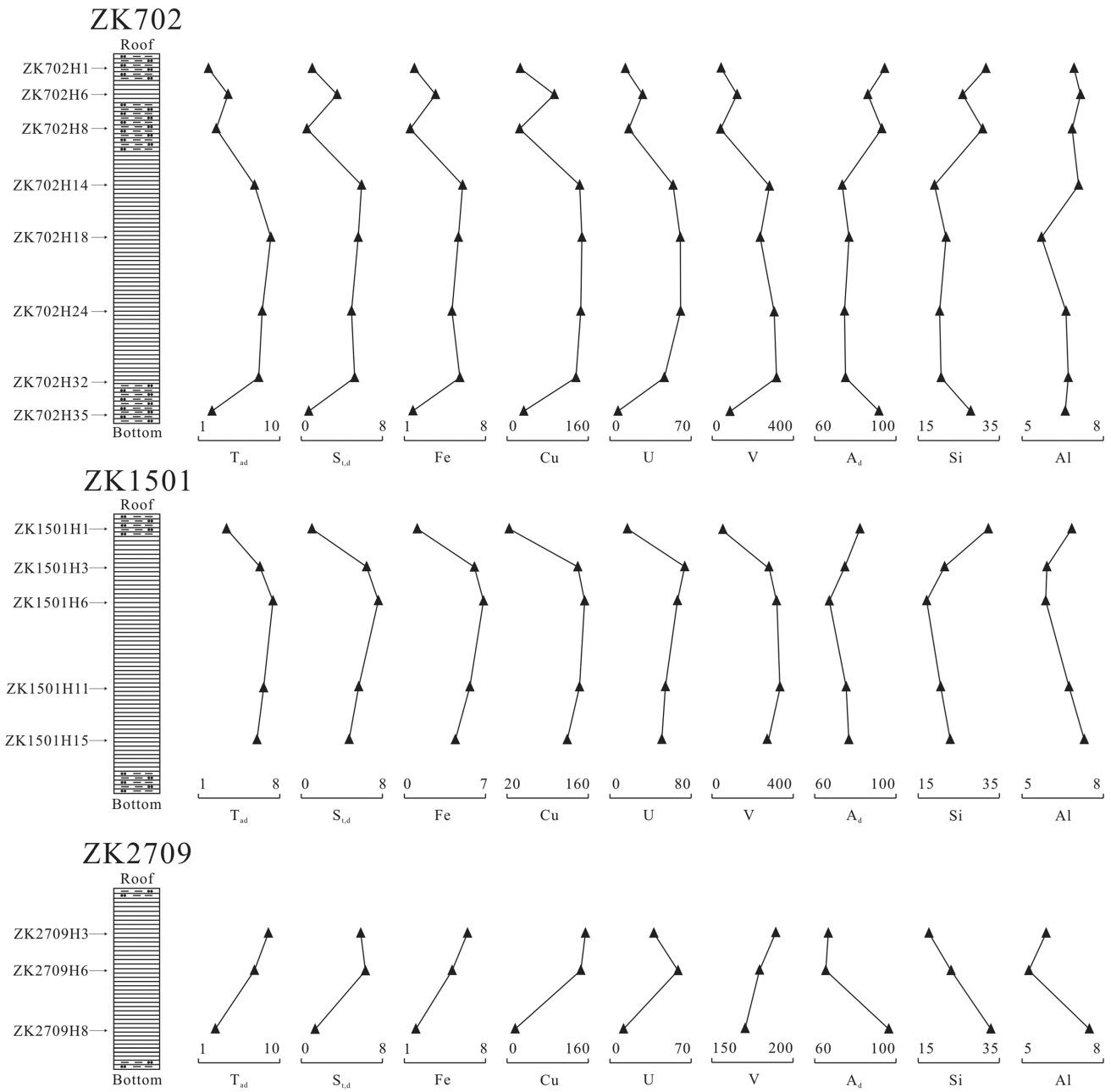

Fig. 9 Vertical variation of oil yield, total sulfur, ash yield, certain trace elements, and major elements in oil shale sections (trace elements in ppm, others in %)

had negative correlation, with values ranging from −0.707 to 0.326) (Table 6). In addition, the elements in this group showed a positive relationship with Al (with the exception of Bi), indicating a terrigenous source.

5.2 Reconstruction of paleoenvironment

Previous studies have suggested that the ratios and calculated values of certain elements can be used to reconstruct lacustrine paleoenvironment (Fan et al. 2012; Bai et al. 2015; Sun et al. 2015; Fu et al. 2016; Jemaï et al. 2016).

The Sr/Cu ratio is sensitive to paleoclimate (Deng and Qian 1993; Fu et al. 2010a, b, c; Liang et al. 2015). Sr/Cu ratios from 1.3 to 5.0 indicate a warm and humid paleoclimate; >5.0, dry and hot. Sr/Cu ratios of our oil shale samples ranged from 1.01 to 12.16, with an average of 3.26 (Table 7), implying that the integral paleoclimate was warm and humid.

The Ba/Al ratio can be used to semiquantitatively reconstruct paleoproductivity of lakes (Dean et al. 1997;

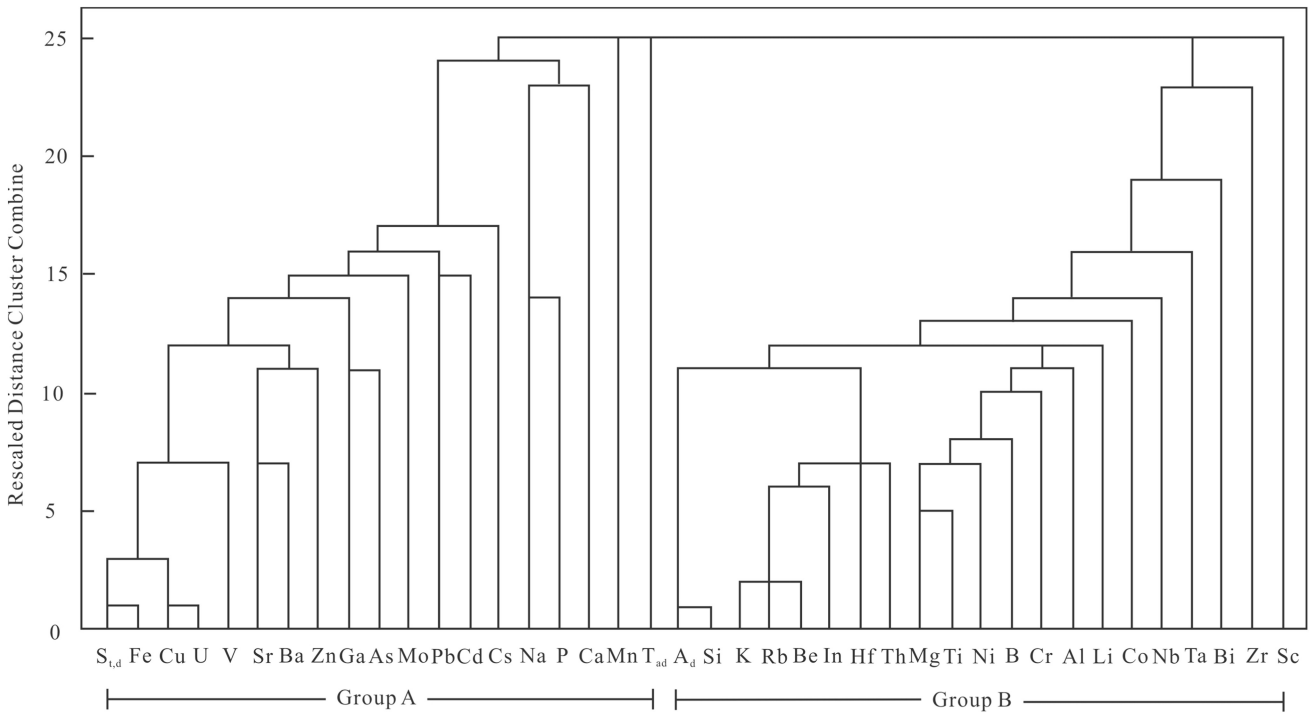

Fig. 10 Cluster analysis of major elements, trace elements, oil yield, ash yield, and total sulfur in oil shale samples (cluster method, Furthest Neighbor; interval, Person correlation; transform values, maximum magnitude of 1)

Luo et al. 2013). Higher values are associated with higher paleoproductivity; a ratio of 0.010 to 0.012 has been designated as high productivity (Dean et al. 1997; Sun et al. 2015). Ba/Al in our samples varied from 0.005 to 0.012, with an average of 0.009 (Table 7), suggesting relatively high paleoproductivity.

The Sr/Ba ratio can be used to reconstruct paleosalinity (Wang et al. 1979, 2014; Wang and Wu 1983; Li and Chen 2003; Guo et al. 2015; Li et al. 2015). Sr/Ba >1, 0.6–1, and <0.6 reflect sea water, brackish water, and fresh water, respectively. Sr/Ba ratios of our samples were generally lower than 1.0 (from 0.27 to 0.69, with an average of 0.38) (Table 7), suggesting that the oil shale mainly formed in fresh water. This could support the opinion that there was no large-scale marine transgression in the southern Ordos Basin during the Triassic (Yin and Lin 1979; Zhang 1984; Zhang et al. 2011; Qiu et al. 2015).

V, Ni, U, and Th are sensitive to redox conditions and V/(V + Ni), U/Th, AU(U-Th/3), and δU(2U/(Th/3 + U)) can reflect paleo-redox conditions (Ernst 1970; Deng and Qian 1993; Jones and Manning 1994; Dypvik and Harris 2001; Teng et al. 2005; Tribovillard et al. 2006; Zhao et al. 2016a, b). V/(V + Ni) <0.5 and δU < 1 both indicate oxidation conditions; V/(V + Ni) >0.5 and δU > 1, reducing conditions (Deng and Qian 1993; Zhao et al. 2016a, 2016b). Strong oxidation conditions are reflected by U/Th < 0.75 and AU <5 ppm; strong reducing conditions by U/Th >1.25 and AU >12 ppm; intermediate values indicate weak oxidation–weak reducing conditions (Qiu et al. 2015; Sun et al. 2015). Average values of V(V + Ni), δU, U/Th, and AU in oil shale samples were 0.88, 1.71, 3.13, and 35.32 ppm, respectively (Table 7), indicating that the Zhangjiatan oil shale was mainly deposited in reducing conditions.

The Fe/Ti ratio can be used to measure hydrothermal influence (Boström 1983; Zhong et al. 2015; Chu et al. 2016). Fe/Ti >20 reflects definite hydrothermal influence, with higher values indicating greater influence (Chu et al. 2016). Six samples (ZK702H14, ZK702H18, ZK702H24, ZK702H32 ZK1501H3, and ZK1501H6) from the eastern study area had Fe/Ti >20 (Table 7), meaning there was hydrothermal influence during oil shale sedimentation. However, three samples (ZK2709H3, ZK2709H6, and ZK2709H8) from the western study area had Fe/Ti <20 (Table 7), indicating less hydrothermal influence.

6 Conclusions

The oil yields of Zhangjiatan oil shale samples ranged from 4.3% to 9.1% (average 6.63%), classifying the oil shale as middle grade.

Minerals in the oil shale were mainly clay minerals, quartz, feldspar, and pyrite (>5%), with illite/smectite dominating the clay minerals. In contrast with marine oil

Table 6 Correlation coefficients of oil yield, calorific value, ash yield, total sulfur, and major elements in oil shale samples

Cases	T_{ad}	A_d	$S_{t,d}$	Si	Al	Mg	Ca	Na	K	P	Mn	Ti	Fe	Cr	Sr	Zr	Ba	Sc	V	Cu	Zn	Ga	As	Pb	Rb	Cs	Th	U	Co	Ni	Nb	Cd	Hf	Ta	Li	Be	In	Bi	Mo	B
T_{ad}	1.000	-0.573	0.395	-0.533	-0.528	-0.182	0.238	0.114	-0.703	0.313	-0.424	-0.186	0.566	0.287	0.156	-0.049	0.055	0.326	0.491	0.523	0.276	-0.162	0.268	-0.402	-0.583	-0.110	-0.707	0.372	0.048	0.139	-0.511	-0.129	-0.547	-0.020	-0.288	-0.603	-0.442	-0.397	0.363	-0.361
A_d		1.000	-0.886	0.954	0.626	0.120	-0.572	0.164	0.792	-0.099	0.277	0.304	-0.890	-0.466	-0.176	0.489	-0.042	0.007	-0.795	-0.817	-0.316	-0.227	-0.503	-0.122	0.762	-0.211	0.557	-0.687	-0.469	-0.112	0.297	-0.420	0.719	0.431	0.462	0.685	0.670	-0.038	-0.145	0.421
$S_{t,d}$			1.000	-0.778	-0.824	-0.420	0.406	-0.227	-0.631	0.037	-0.428	-0.543	0.956	0.185	0.067	-0.531	-0.217	-0.310	0.726	0.914	0.261	0.330	0.544	0.349	-0.583	0.335	-0.286	0.866	0.299	-0.228	-0.340	0.603	-0.687	-0.655	-0.573	-0.564	-0.761	0.360	0.287	-0.631
Si				1.000	0.433	-0.067	-0.546	0.210	0.743	0.007	0.229	0.090	-0.814	-0.652	-0.127	0.600	-0.071	-0.198	-0.757	-0.682	-0.305	-0.210	-0.377	-0.022	0.768	-0.133	0.607	-0.526	-0.609	-0.294	0.281	-0.267	0.742	0.295	0.285	0.678	0.588	0.057	0.020	0.247
Al					1.000	0.585	-0.288	-0.018	0.573	-0.195	0.538	0.671	-0.786	0.176	-0.019	0.276	0.342	0.334	-0.490	-0.825	-0.064	-0.033	-0.409	-0.176	0.436	-0.130	0.260	-0.827	0.189	0.480	0.443	-0.411	0.566	0.554	0.730	0.555	0.768	-0.311	-0.461	0.784
Mg						1.000	0.326	0.063	0.066	-0.005	0.544	0.890	-0.444	0.599	-0.206	-0.175	0.161	0.502	-0.365	-0.607	-0.461	-0.552	-0.638	-0.585	-0.174	-0.393	-0.219	-0.661	0.390	0.838	0.418	-0.537	0.117	0.694	0.378	-0.088	0.271	-0.350	-0.801	0.794
Cu							1.000	0.402	-0.694	0.599	0.482	0.188	0.332	0.375	0.498	-0.212	0.388	0.340	0.434	0.409	0.131	-0.240	-0.021	-0.054	-0.754	-0.238	-0.711	0.277	0.291	0.316	-0.247	0.373	-0.579	-0.133	-0.535	-0.736	-0.587	-0.344	-0.061	-0.119
Na								1.000	-0.354	0.737	0.438	0.236	-0.210	-0.247	0.500	0.146	0.491	0.308	0.009	0.005	0.054	-0.427	-0.341	-0.193	-0.339	-0.327	-0.398	0.033	-0.291	0.030	-0.482	-0.010	-0.086	0.139	-0.271	-0.366	-0.293	-0.227	0.245	-0.091
K									1.000	-0.444	0.158	0.116	-0.660	-0.361	-0.454	0.315	-0.293	-0.312	-0.760	-0.738	-0.373	0.024	-0.244	0.046	0.936	0.078	0.853	-0.666	-0.223	-0.126	0.653	-0.252	0.820	0.382	0.535	0.936	0.831	0.275	-0.375	0.392
P										1.000	0.525	0.103	0.060	-0.134	0.573	0.233	0.431	0.161	0.136	0.248	0.211	-0.373	-0.101	-0.122	-0.446	-0.206	-0.465	0.174	-0.020	0.150	-0.324	0.292	-0.177	0.037	-0.388	-0.391	-0.313	-0.330	0.290	-0.209
Mn											1.000	0.555	-0.477	0.063	0.416	0.280	0.569	0.245	-0.238	-0.395	-0.006	-0.258	-0.325	-0.088	-0.004	-0.170	-0.077	-0.477	0.157	0.423	0.271	0.148	0.255	0.366	0.045	0.130	0.289	-0.318	-0.338	0.399
Ti												1.000	-0.497	0.584	-0.125	-0.124	0.228	0.559	-0.374	-0.643	-0.303	-0.521	-0.736	-0.647	-0.150	-0.335	-0.225	-0.678	0.390	0.845	0.165	-0.539	0.101	0.701	0.511	-0.029	0.247	-0.359	-0.625	0.843
Fe													1.000	0.266	0.116	-0.469	-0.124	-0.192	0.799	0.918	0.393	0.357	0.601	0.204	-0.616	0.394	-0.388	0.825	0.311	-0.155	-0.459	0.521	-0.737	-0.571	-0.521	-0.556	-0.718	0.254	0.363	-0.632
Cr														1.000	-0.090	-0.432	0.106	0.492	0.294	0.023	0.082	-0.082	-0.151	-0.460	-0.541	-0.050	-0.545	-0.134	0.763	0.800	-0.067	-0.196	-0.454	0.227	0.290	-0.392	-0.183	-0.345	-0.406	0.504
Sr															1.000	0.420	0.852	0.316	0.595	0.383	0.789	0.368	0.429	0.309	-0.372	0.129	-0.525	0.304	-0.125	-0.154	-0.535	0.555	-0.394	-0.426	-0.489	-0.320	-0.270	-0.492	0.606	-0.362
Zr																1.000	0.468	-0.063	-0.170	-0.298	0.278	0.107	0.254	-0.036	0.417	0.173	0.124	-0.296	-0.569	-0.234	0.094	0.046	0.410	0.072	-0.082	0.452	0.486	-0.386	0.403	0.012
Ba																	1.000	0.394	0.427	0.027	0.629	0.248	0.270	-0.001	-0.318	0.205	-0.465	-0.050	-0.031	0.179	-0.304	0.245	-0.170	-0.045	-0.219	-0.140	0.034	-0.507	0.310	0.029
Sc																		1.000	0.090	-0.189	0.159	-0.280	-0.347	-0.434	-0.336	-0.599	-0.702	-0.344	0.142	0.483	-0.340	-0.436	-0.363	0.341	0.142	-0.433	-0.054	-0.823	-0.170	0.267
V																			1.000	0.847	0.767	0.590	0.722	0.301	-0.696	0.448	-0.600	0.760	0.221	-0.139	-0.646	0.590	-0.808	-0.681	-0.553	-0.597	-0.658	-0.089	0.577	-0.553
Cu																				1.000	0.536	0.419	0.655	0.425	-0.609	0.310	-0.423	0.944	0.131	-0.365	-0.588	0.682	-0.736	-0.764	-0.666	-0.613	-0.796	0.157	0.604	-0.790
Zn																					1.000	0.736	0.694	0.399	-0.276	0.442	-0.379	0.437	0.116	-0.189	-0.581	0.588	-0.452	-0.580	-0.242	-0.156	-0.224	-0.318	0.717	-0.394
Ga																						1.000	0.795	0.712	0.108	0.690	0.180	0.435	0.072	-0.456	-0.184	0.612	-0.194	-0.720	-0.123	0.207	-0.018	0.195	0.505	-0.376
As																							1.000	0.507	-0.100	0.697	-0.049	0.598	-0.103	-0.491	-0.207	0.638	-0.304	-0.668	-0.500	0.000	-0.157	0.112	0.624	-0.656
Pb																								1.000	0.191	0.280	0.357	0.512	-0.032	-0.649	-0.012	0.725	-0.020	-0.783	-0.241	0.132	-0.129	0.343	0.387	-0.508
Rb																									1.000	0.008	0.844	-0.540	-0.385	-0.355	0.561	-0.200	0.822	0.234	0.453	0.915	0.789	0.217	-0.169	0.188
Cs																										1.000	0.269	0.371	0.026	-0.251	-0.041	0.510	-0.066	-0.422	-0.213	0.286	0.009	0.498	0.383	-0.234
Th																											1.000	-0.265	-0.108	-0.369	0.636	-0.002	0.778	0.063	0.372	0.854	0.600	0.660	-0.211	0.125
U																												1.000	-0.001	-0.500	-0.575	0.658	-0.662	-0.851	-0.669	-0.561	-0.812	0.332	0.662	-0.784
Co																													1.000	0.698	0.140	0.112	-0.209	0.084	0.428	-0.182	-0.100	-0.031	-0.415	0.401
Ni																														1.000	0.232	-0.426	-0.010	0.654	0.499	-0.160	0.163	-0.391	-0.624	0.755
Nb																															1.000	-0.234	0.736	0.462	0.419	0.625	0.722	0.210	-0.700	0.474
Cd																																1.000	-0.319	-0.770	-0.547	-0.109	-0.406	0.255	0.501	-0.565
Hf																																	1.000	0.518	0.563	0.856	0.850	0.208	-0.359	0.434
Ta																																		1.000	0.551	0.292	0.586	-0.240	-0.700	0.677
Li																																			1.000	0.524	0.624	-0.069	-0.497	0.776
Be																																				1.000	0.869	0.286	-0.194	0.312
In																																					1.000	-0.086	-0.408	0.515
Bi																																						1.000	-0.056	-0.226
Mo																																							1.000	-0.672
B																																								1.000

Table 7 Parameters of paleoenvironment

Sample no.	Sr/Cu	Ba/Al	Sr/Ba	V/(V + Ni)	U/Th	AU	δU	Fe/Ti
ZK702H1	7.23	0.008	0.30	0.79	0.46	3.50	1.16	9.55
ZK702H6	1.22	0.005	0.29	0.85	1.28	21.10	1.59	18.12
ZK702H8	5.61	0.008	0.22	0.83	0.51	5.70	1.21	5.54
ZK702H14	1.16	0.007	0.31	0.89	3.63	49.13	1.83	24.62
ZK702H18	1.59	0.008	0.50	0.89	5.68	57.70	1.89	25.39
ZK702H24	2.71	0.012	0.50	0.92	6.39	57.91	1.90	24.06
ZK702H32	2.48	0.012	0.41	0.92	3.70	42.77	1.83	27.18
ZK702H35	17.53	0.013	0.61	0.85	0.65	3.30	1.32	3.46
ZK1501H1	5.32	0.007	0.30	0.83	0.52	5.90	1.22	7.89
ZK1501H3	1.33	0.009	0.33	0.90	4.32	62.93	1.86	23.81
ZK1501H6	1.01	0.007	0.35	0.90	4.90	57.50	1.87	30.10
ZK1501H11	3.09	0.011	0.57	0.91	5.13	47.78	1.88	19.26
ZK1501H15	3.45	0.011	0.50	0.89	3.13	42.27	1.81	17.26
ZK2709H3	1.97	0.009	0.30	0.84	1.35	13.33	1.60	14.00
ZK2709H6	1.90	0.009	0.30	0.83	1.80	17.60	1.69	12.12
ZK2709H8	2.77	0.008	0.27	0.82	0.91	8.03	1.46	6.91
Average	3.77	0.009	0.38	0.87	2.77	31.03	1.63	16.83

shale, quartz, feldspar, and clay minerals in lacustrine oil shale were clearly higher while calcite content was much lower. Si mainly occurred in quartz and in clay minerals. Fe was mainly associated with organic matter and barely present in the clay minerals, which is opposite to marine oil shale. Ca occurred in various forms.

According to cluster analysis, Fe, Cu, U, V, Sr, Ba, Zn, Ga, As, Mo, Pb, Cd, Cs, Na, P, Ca, and Mn were generally associated with organic matter, while Si, K, Rb, Be, In, Hf, Th, Mg, Ti, Ni, B, Cr, Al, Li, Co, Nb, Ta, Bi, Zr, and Sc were not; all showed a positive relationship with Al (with the exception of Bi), indicating these elements are closely associated with a terrigenous source.

The Sr/Cu ratio of oil shale samples ranged from 1.01 to 12.16, with an average of 3.26, indicating a warm and humid paleoclimate. Ba/Al was between 0.005 and 0.012, suggesting that paleoproductivity was high. Sr/Ba varied from 0.27 to 0.69, suggesting that the oil shale was mainly deposited in fresh water and there was no large-scale marine transgression in the southern Ordos Basin. The average values of V/(V + Ni), U/Th, AU, and δU of oil shale samples were 0.88, 3.13, 35.32 ppm, and 1.71, respectively, indicating that the shale was mainly deposited under reducing conditions. The Fe/Ti ratio of the six oil shale samples from the southern study area was >20, indicating clear hydrothermal influence; the ratio of samples from the western study area was <20, suggesting lesser hydrothermal influence.

Acknowledgements This work was supported by funding from the National Natural Science Foundation of China (No. 41173055) and the Fundamental Research Funds for the Central Universities (No. 310827172101).

References

Bai YL, Wu WJ (2006) The resource characteristics of oil shale and analysis of condition of prospecting and using in Minhe Basin, west China. Nat Gas Geosci 17(5):627–633 **(in Chinese with English Abstract)**

Bai YL, Ma L, Wu WJ, Ma YL (2009) Geological characteristics and resource potential of oil shale in Ordos basin. Geol China 36(5):1123–1137 **(in Chinese with English abstract)**

Bai Y, Liu Z, Sun P, Liu R, Hu X, Zhao H, Xu Y (2015) Rare earth and major element geochemistry of Eocene fine-grained sediments in oil shale- and coal-bearing layers of the Meihe Basin, Northeast China. J Asian Earth Sci 97(97):89–101

Bian LZ, Zhang SC, Zhang BM, Wang DR (2005) Red algal fossils discovered from the Neoproterozoic xiamaling oil shales, Xiahuayuan town of Hebei province. Acta Micropalaeontologica Sin 22(3):209–216 **(in Chinese with English abstract)**

Boström K (1983) Genesis of ferromanganese deposits-diagnostic criteria for recent and old deposits. In: Rona PA, Boström K, Laubier L, Smith KL (eds) Hydrothermal processes at seafloor spreading centers. Springer, New York, pp 473–489

Cao J, Wu M, Chen Y, Hu K, Bian LZ, Wang LG, Zhang Y (2012) Trace and rare earth element geochemistry of Jurassic mudstones in the northern Qaidam Basin, northwest China. Chem Erde-Geochem 72:245–252

Chang Y, Liu RH, Bai WH, Sun SS (2012) Geologic characteristic and regular pattern of Triassic oil shale south of Ordos Basin. China Pet Explor 2:74–78 **(in Chinese)**

Chen JF, Sun XL (2004) Preliminary study of geochemical characteristics and formation of organic matter rich stratigraphy of Xiamaling-Formation of later Proterozoic in north China. Nat Gas Geosci 15(2):110–114 **(in Chinese with English Abstract)**

Chen JF, Sun XL, Liu WH, Zheng JJ (2004) Geochemical characteristics of organic matter-rich strata of lower Cambrian in Tarim Basin and its origin. Sci China Ser D Earth Sci 34(S1):107–113 **(in Chinese with English Abstract)**

Chu CL, Chen QL, Zhang B, Shi Z, Jiang HJ, Yang X (2016) Influence on formation of Yuertusi source rock by hydrothermal activities at Dongergou section. Tarim Basin. Acta Sedimentologica Sinica 34(4):803–810 **(in Chinese with English abstract)**

Dean WE, Gardner JV, Piper DZ (1997) Inorganic geochemical indicators of glacial-interglacial changes in productivity and anoxia on the California continental margin. Geochim Cosmochim Acta 61:4507–4518

Deng HW, Qian K (1993) Sedimentary Geochemistry and Environmental Analysis. Gansu science and technology press, Lanzhou **(in Chinese)**

Deng NT, Zhang ZH, Ren LY, Wang FB, Liang QS, Li YX, Li WH, Zhao SF, Luo MJ (2013) Geochemical characteristics and distribution rules of oil shale from Yanchang Formation Southern Ordos Basin. Pet Geol Exp 35(4):432–437 **(in Chinese with English abstract)**

Dong QS, Wang LX, Yu WX (2006) The key parameters of oil-shale resource appraisement and its evaluating methods. J Jilin Univ 36(6):899–903 **(in Chinese with English abstract)**

Dong LH, An SJ, Wang BY (2014) Relationship between distribution of hydrocarbon source rocks and oil-gas enrichment of Yanchang Formation, Triassic Ordos Basin. Unconv Oil Gas 1:17–21 **(in Chinese with English abstract)**

Dypvik H, Harris NB (2001) Geochemical facies analysis of fine grained siliciclastics using Th/U, Zr/Rb and (Zr+ Rb)/Sr ratios. Chem Geol 181:131–146

Ernst TW (1970) Geochemical facies analysis. Elsevier, Amsterdam

Fan YH, Qu HJ, Wang H, Yang XC, Feng YW (2012) The application of trace elements analysis to identifying sedimentary media environment: a case study of Late Triassic strata in the middle part of western Ordos Basin. Geol China 39(2):382–389 **(in Chinese with English abstract)**

Fu XG, Wang J, Wang ZJ, Chen WX (2007) Biomarkers and sedimentary environment of Late Jurassic marine oil shale in Qiangtang basin, northern Xizang and its geological significance. Geochimica 36(5):486–496 **(in Chinese with English abstract)**

Fu X, Jian W, Zeng Y, Li Z, Wang Z (2009) Geochemical and palynological investigation of the Shengli River marine oil shale (China): implications for paleoenvironment and paleoclimate. Int J Coal Geol 78(3):217–224

Fu SQ, Zhu ZY, Ou YTP, Qiu Y (2010a) Sedimentary records of rare earth elements from southern South China Sea continental slope and Its paleoclimatic implications during late Quaternary. Trop Geogr 30(1):24–29 **(in Chinese with English abstract)**

Fu XG, Wang J, Zeng Y, Tan F, Chen W, Feng X (2010b) Geochemistry of rare earth elements in marine oil shale-a case study from the Bilong Co area, Northern Tibet,China. Oil Shal 27(3):194–208

Fu XG, Wang J, Zeng Y, Tan F, Feng X (2010c) REE geochemistry of marine oil shale from the Changshe Mountain area, northern Tibet, China. Int J Coal Geol 81(3):191–199

Fu X, Wang J, Tan F, Feng X, Wang D (2015) Occurrence and enrichment of trace elements in marine oil shale (China) and their behaviour during combustion. Oil Shale 32(1):42–65

Fu XG, Wang J, Feng XL, Chen WB, Wang D, Song CY, Zeng SQ (2016) Mineralogical composition of and trace-element accumulation in lower Toarcian anoxic sediments: a case study from the Bilong Co. Oil shale, eastern Tethys. Geol Mag 153(4):618–634

GB/T 14506.1 ~ 14-2010 (2010) Methods for chemical analysis of silicate rocks. (**in Chinese**)

GB/T 14506.30-2010 (2010) Methods for chemical analysis of silicate rocks-part 30: determination of 44 elements (**in Chinese**)

GB/T 212-2008 (2008) Proximate analysis of coal (**in Chinese**)

GB/T 213-2008 (2008) Determination of calorific value of coal (**in Chinese**)

GB/T 6730.17-2014 (2014) Iron ores-Determination of sulfur content-Combustion iodometric method (**in Chinese**)

Guo LY, Li ZS, Xie XN, Shang SF, Fan ZH, Liu ZJ, Wu F (2015) High-frequency variation of geochemical elements and its geological implication on lacustrine organic-rich mudstone and shale formation: an example from the core-taking segment of well BY1 in the Biyang depression. Geoscience 29(6):1360–1370 **(in Chinese with English abstract)**

Hakimi MH, Wan HA, Alqudah M, Makeen YM, Mustapha KA (2016) Organic geochemical and petrographic characteristics of the oil shales in the Lajjun area, Central Jordan: origin of organic matter input and preservation conditions. Fuel 181:34–45

He ZX (2003) Evolution history and petroleum of the Ordos Basin. Petroleum Industry Press (**in Chinese with English Abstract**)

Jemaï MBM, Yaakoub NK, Sdiri A, Azouzi R, Cherni R, Aissa LB, Dupaly J (2016) Reconstruction of the late cretaceous-paleocene paleoenvironment (northern tunisia) from biostratigraphy, geochemistry and clay mineralogy. Arab J Geosci 9(2):1–12

Jones B, Manning DAC (1994) Comparison of geochemical indices used for the interpretation of depositional environments in ancient mudstones. Chem Geol 111(1–4):112–129

Li JL, Chen DJ (2003) Summary of quantified research method on paleosalinity. Pet Geol Recovery Effic 10(5):1–3 **(in Chinese with English abstract)**

Li RX, Xi SL, Di LJ (2006) Oil/gas reservoiring phases determined through petrographic analysis of hydrocarbon inclusions in reservoirs: taking Longdong oilfield, Ordos basin, as an example. Oil Gas Geol 27(2):194–199 **(in Chinese with English abstract)**

Li W, Pang J, Cao H (2009a) Depositional system and paleogeographic evolution of the late Triassic Yanchang Stage in Ordos Basin. J Northwest Univ 39(3):501–506 **(in Chinese with English abstract)**

Li YH, Li JC, Jiang T, Wei JS, Lu JC, Hang J (2009b) Characteristics of the Triassic oil shale in the Hejiafang area, Ordos Basin. J Jilin Univ (Earth Sci Ed) 39(1):65–71 **(in Chinese with English abstract)**

Li YH, Jiang T, Wu FL, Zhang HY, Yao ZG, Wang BW (2014) Evaluation methods and results of oil shale resources in southeastern Ordos Basin. Geol Bull China 9:1417–1424 **(in Chinese with English abstract)**

Li ZC, Li WH, Lai SC, Li YX, Li YH, Shang T (2015) The palaeosalinity analysis of Paleogene lutite in Weihe Basin. Acta Sedimentol Sin 33(3):480–485 **(in Chinese with English abstract)**

Li D, Li R, Wang B, Liu Z, Wu X, Liu F, Zhao B, Cheng J, Kang W (2016) Study on oil–source correlation by analyzing organic geochemistry characteristics: a case study of the Upper Triassic Yanchang Formation in the south of Ordos Basin. China. Acta Geochimica 35(4):1–13

Liang WJ, Xiao CT, Xiao K, Lin W (2015) The relationship of Late Jurassic paleoenvironment and paleoclimate with geochemical elements in Amdo Country of northern Tibet. Geol China 42(4):1079–1091 **(in Chinese with English abstract)**

Liu ZJ, Liu R (2005) Oil shale resource state and evaluating system. Earth Sci Front 12(3):315–323 **(in Chinese with English abstract)**

Liu ZJ, Dong QS, Ye SQ, Zhu JW, Guo W, Li DC, Liu R, Zhang HL, Du JF (2006) The situation of oil shale resources in China. J Jilin Univ (Earth Sci Ed) 36(6):869–876 **(in Chinese with English abstract)**

Liu CY, Zhao HG, Zhao JF, Wang JQ, Zhang DD, Yang MH (2008) Temporo-spatial coordinates of evolution of the Ordos Basin and its mineralization responses. Acta Geol Sin 82(6):1229–1243

Liu ZJ, Yang HL, Dong QS, Zhu JW, Guo W, Ye SQ, Liu R, Meng QT, Zhang HL, Gan SC (2009) Oil Shale in China. Petroleum Industry Press, Beijing

Liu Y, Zhong NN, Song T, Tian YJ, Han H, Zhu L (2011) Kinetics of marine oil shale: a case study of Xiamaling Formation oil shale in Yanshan region, North China. J Jilin Univ (Earth Sci Ed) 41(s1):78–84 **(in Chinese with English abstract)**

Liu R, Liu Z, Guo W, Chen H (2015) Characteristics and comprehensive utilization potential of oil shale of the Yin'e basin, inner Mongolia, China. Oil Shale 32(4):293–312

Lu JC, Li YH, Wei XY, Wei JS (2006) Research on the depositional environment and resources potential of the oil shale in the chang 7 member, Triassic Yanchang Formation in the Ordos Basin. J Jilin Univ (Earth Sci Ed) 36(6):928–932 **(in Chinese with English abstract)**

Lü DW, Li ZX, Liu HY, Li Y, Feng TT, Wang DD, Wang PL, Li SY (2015) The characteristics of coal and oil shale in the coastal sea areas of Huangxian Coalfield. East China. Oil Shale 32(3):204–207

Luo QY, Zhong NN, Zhu L, Wang YN, Qin J, Qi L, Zhang Y, Ma Y (2013) Correlation of burial organic carbon and paleoproductivity in the Mesoproterozoic Hongshuizhuang Formation, northern North China. Chin Sci Bul 11:1036–1047 **(in Chinese)**

Luo YS, Zhang SN, Zhang ZH, Deng NT, He YH, Liang QS (2014) Favorable area forecast of oil shale exploration in southern Ordos basin. China Min Mag 1:83–86 **(in Chinese with English abstract)**

Ma ZH, Chen QS, Shi ZW, Wang C, Du WG, Zhao CY (2016) Geochemistry of oil shale from chang 7 reservoir of Yanchang Formation in south Ordos Basin and its geological significance. Geol Bull China 35(9):1550–1558 **(in Chinese with English abstract)**

Mclennan SM (2001) Relationships between the trace element composition of sedimentary rocks and upper continental crust. Geochem Geophys Geosyst 2(4):203–236

Mukhopadhyay PK, Goodarzi F, Crandlemire AL, Gillis KS, Macneil DJ, Smith WD (1998) Comparison of coal composition and elemental distribution in selected seams of the Sydney and Stellarton Basins, Nova Scotia, Eastern Canada. Int J Coal Geol 37(1–2):113–141

Qiu XW, Liu CY, Mao GZ, Yu D (2010) Enrichment feature of thorium element in tuff interlayers of Upper Triassic Yanchang Formation in Ordos basin. Geol Bull China 29(8):1185–1191 **(in Chinese with English abstract)**

Qiu X, Liu C, Mao G, Deng Y, Wang F, Wang J (2014) Late Triassic tuff intervals in the Ordos basin, Central China: their depositional, petrographic, geochemical characteristics and regional implications. J Asian Earth Sci 80:148–160

Qiu XW, Liu CY, Wang FF, Deng Y, Mao GZ (2015) Trace and rare earth element geochemistry of the Upper Triassic mudstones in the southern Ordos Basin, Central China. Geol J 50:399–413

SH/T 0508-1992 (1992) The test method for oil yield from oil shale-The method of low temperature carbonization (**in Chinese**)

Song Y, Liu Z, Meng Q, Xu J, Sun P, Cheng L, Zheng G (2016) Multiple controlling factors of the enrichment of organic matter in the upper cretaceous oil shale sequences of the Songliao Basin, NE China: implications from geochemical analyses. Oil Shale 33(2):142–166

Sun ZC, Yang P, Zhang ZH (1997) Seolmentirry Enuironments and Hydrocarbon Generation of Cenoaoic Salified Lakes in China. Petroleum Industry Press (**in Chinese**)

Sun SL, Chen JF, Liu WH, Zhang SC, Wang DR (2003) Hydrothermal venting on the Seafloor and formation of organic-rich sediments -evidence from the Neoproterozoic Xiamaling Formation, North China. Geol Rev 49(6):588–595 **(in Chinese with English abstract)**

Sun SS, Yao YB, Lin W (2015) Elemental geochemical characteristics of the oil shale and the Paleo-Lake environment of the Tongchuan area, southern Ordos Basin. Bull Mineral Petrol Geochem 34(3):642–645 **(in Chinese with English abstract)**

SY/T 6210-1996 (1996) Oil and gas standard of P.R. China: X-ray diffraction quantitative analysis methods of the clay minerals and common non-clay minerals in sedimentary rocks (**in Chinese**)

Teng GE, Hui LW, Xu YC, Chen JF (2005) Correlative study on parameters of inorganic geochemistry and hydrocarbon source rocks formative environment. Adv Earth Sci 20(2):193–200 **(in Chinese with English abstract)**

Tribovillard N, Algeo TJ, Lyons T, Riboulleau A (2006) Trace metals as paleoredox and paleoproductivity proxies-an update. Chem Geol 232(1–2):12–32

Wan YS, Xie HQ, Yang H, Wang AJ, Liu DY, Kröner A, Wilde SA, Geng YS, Sun LY, Ma MZ, Liu SJ, Dong CY, Du LL (2013) Is the ordos block archean or paleoproterozoic in age? Implications for the precambrian evolution of the North China craton. Am J Sci 313:683–711

Wang YY, Wu P (1983) Geochemical criteria of sediments in the coastal area of Jiangsu and Zhejiang Provinces. J Tongji Univ (Nat Sci) 4:82–90 **(in Chinese with English abstract)**

Wang YD, Yan QB (2012) The resource application prospects of Zhangjiatan shale, Southern Ordos Basin. J Northwest Univ (Nat Sci Ed) 42(3):453–458 **(in Chinese with English abstract)**

Wang YY, Guo WY, Zhang GD (1979) Application of some geochemical indicators in determing of sedimentary environment of the Funing Group(Paleogene), Jin-Hu Depression, Kiangsu Provience. J Tongji Univ 7(2):51–60 **(in Chinese with English abstract)**

Wang J, Fu XG, Li ZX, Xiong S (2010) Formation and significance of the oil shales from the North Qiantang Basin. Sediment Geol Tethyan Geol 30(3):11–17 **(in Chinese with English abstract)**

Wang CY, Zheng RC, Liu Z, Liang XW, Li TY, Zhang JW, Li YN (2014) Paleosalinity of chang 9 reservoir in Longdong area, Ordos basin and its geological significance. Acta Sedimentol Sin 32(1):159–165 **(in Chinese with English abstract)**

Wei D, Ma ZH, Chen QS (2016) Mesozoic–Cenozoic structure characteristics and coexisting relationships of multiple energy minerals in Weibei uplift of Ordos Basin. J Earth Sci Environ 38(3):355–364 **(in Chinese with English abstract)**

Wu FL, Li WH, Li YH, Xi SL (2004) Delta sediments and evolution of the Yanchang Formation of upper Triassic in Ordos Basin. J Palaeogeogr 6(3):307–315 **(in Chinese with English abstract)**

Xie SK, Du BW, Wang J, Dong Y (2014) Geochemical characteristics of oil shale member of Dingqinghu Formation in Lunpola Basin of Tibet and their geological implications. Acta Petrologica Et Mineralogica 33(3):503–510 **(in Chinese with English abstract)**

Yang H, Zhang WZ, Wu K, Li SP, Peng PA, Qin Y (2010) Uranium enrichment in lacustrine oil source rocks of the Chang 7 member of the Yanchang Formation, Ordos Basin. China. J. Asian Earth Sci 39:285–293

Yin HF, Lin HM (1979) Triassic marine strata in Weibei area of the southern Ordos basin: implications for the epoch of Shiqianfeng Formation. Acta Stratigraphica Sin 3(4):233–241 **(in Chinese)**

Yu ZL, Zhu HY (2013) The Oil Shale sedimentary characteristics in Jiufotang Formation of Jianchang Basin in the western Liaoning Province. J Oil Gas Technol 35(1):53–57 **(in Chinese with English abstract)**

Yuan W, Liu G, Stebbins A, Xu L, Niu X, Luo W, Li C (2016) Reconstruction of redox conditions during deposition of organic-rich shales of the Upper Triassic Yangchang Formation, Ordos Basin, China. Palaeogeography Palaeoclimatology Palaeoecology (**in press**)

Zeng SQ, Wang J, Fu XG, Feng XL, Sun W (2013) Hydrocarbon generation potential and sedimentary environment for the source rocks along the Changshe Mountain oil shale section in North Qiangtang Basin. Geol China 40(6):1861–1871 **(in Chinese with English abstract)**

Zeng SQ, Wang J, Fu XG, Feng XL, Feng WB, Sun W (2014) Characteristic and formation condition of the Cretaceous marine oil shale in the Qiangtang Basin. Geol Rev 60(2):449–463 **(in Chinese with English abstract)**

Zhang K (1984) The Triassic marine strata of south margin of Ordos basin and discussions on some problems concerned. Chin Sci Bull 29(2):233–236 **(in Chinese with English abstract)**

Zhang XJ, Fan YF, Zhang JJ, Wang GC (2004) Microelement and geologic significance of Yanchang Formation in Fuxian area, Ordos Basin. Xinjiang Pet Geol 25(5):483–485 **(in Chinese with English abstract)**

Zhang CL, Gao AL, Liu Z, Huang J, Yang YJ, Zhang Y (2011) Study of character on sedimentary water and palaeoclimate for Chang7 member in Ordos Basin. Nat GAS Geosci 22(4):582–587 **(in Chinese with English abstract)**

Zhang QC, Wang KM, Luo SS, Wu XZ (2013) Study on the characteristics and origin of the oil shale in the chang 7 member, Yanchang Formation in Ordos Basin. Adv Geosci 03(4):197–209 **(in Chinese with English abstract)**

Zhao Y, Yao JL, Duan Y, Wu YZ, Cao XX, Xu L, Chen SS (2015) Oil-source analysis for chang-9 subsection(Upper Triassic) of Eastern Gansu Province in Ordos Basin. Acta Sedimentol Sin 33(5):1023–1032 **(in Chinese with English abstract)**

Zhao BS, Li RX, Wang XZ, Wu XY, Wang N, Qin XL, Cheng JH, Li JJ (2016a) Sedimentary environment and preservation conditions of organic matter analysis of Shanxi Formation mud shale in Yanchang exporation area, Ordos Basin. Geol Sci Technol Inf 35(6):103–111 **(in Chinese with English abstract)**

Zhao J, Jin Z, Jin Z, Geng Y, Wen X, Yan C (2016b) Applying sedimentary geochemical proxies for paleoenvironment interpretation of organic-rich shale deposition in the Sichuan Basin, China. Int J Coal Geol 163:52–71

Zhong DK, Jiang ZK, Guo Q, Sun HT (2015) A review about research history, situation and prospects of hydrothermal sedimentation. J Palaeogeogr 17(3):285–296 **(in Chinese with English abstract)**

Zhu YH, Tai SC, Sun YY (2000) Application of Mathematical Statistics. Wuhan University of Hydraulic and Electric Engineering Press, Wuhan

Zou C, Wang L, Li Y, Tao S, Hou L (2012) Deep-lacustrine transformation of sandy debrites into turbidites, Upper Triassic, Central China. Sediment Geol 265–266(15):143–155